Title
"Caged calcium" in Aplysia pacemaker neurons. Characterization of calcium-activated potassium and nonspecific cation currents.

Journal
The Journal of General Physiology, 93(6)

ISSN
0022-1295

Authors
Landò, L
Zucker, RS

Publication Date
1989-06-01

DOI
10.1085/jgp.93.6.1017

Peer reviewed

"Caged Calcium" in *Aplysia* Pacemaker Neurons

Characterization of Calcium-activated Potassium and Nonspecific Cation Currents

LUCA LANDÒ and ROBERT S. ZUCKER

From the Department of Physiology-Anatomy, University of California, Berkeley, California 94720

ABSTRACT We have studied calcium-activated potassium current, $I_{K(Ca)}$, and calcium-activated nonspecific cation current, $I_{NS(Ca)}$, in *Aplysia* bursting pacemaker neurons, using photolysis of a calcium chelator (nitr-5 or nitr-7) to release "caged calcium" intracellularly. A computer model of nitr photolysis, multiple buffer equilibration, and active calcium extrusion was developed to predict volume-average and front-surface calcium concentration transients. Changes in arsenazo III absorbance were used to measure calcium concentration changes caused by nitr photolysis in microcuvettes. Our model predicted the calcium increments caused by successive flashes, and their dependence on calcium loading, nitr concentration, and light intensity. Flashes also triggered the predicted calcium concentration jumps in neurons filled with nitr-arsenazo III mixtures. In physiological experiments, calcium-activated currents were recorded under voltage clamp in response to flashes of different intensity. Both $I_{K(Ca)}$ and $I_{NS(Ca)}$ depended linearly without saturation upon calcium concentration jumps of 0.1–20 μM. Peak membrane currents in neurons exposed to repeated flashes first increased and then declined much like the arsenazo III absorbance changes in vitro, which also indicates a first-order calcium activation. Each flash-evoked current rose rapidly to a peak and decayed to half in 3–12 s. Our model mimicked this behavior when it included diffusion of calcium and nitr perpendicular to the surface of the neuron facing the flashlamp. Na/Ca exchange extruding about 1 pmol of calcium per square centimeter per second per micromolar free calcium appeared to speed the decline of calcium-activated membrane currents. Over a range of different membrane potentials, $I_{K(Ca)}$ and $I_{NS(Ca)}$ decayed at similar rates, indicating similar calcium stoichiometries independent of voltage. $I_{K(Ca)}$, but not $I_{NS(Ca)}$, relaxes exponentially to a different level when the voltage is suddenly changed. We have estimated voltage-dependent rate constants for a one-step first-order reaction scheme of the activation of $I_{K(Ca)}$ by calcium. After a depolarizing pulse, $I_{NS(Ca)}$ decays at a rate that is well predicted by a model of diffusion of calcium away from the inner membrane surface after it has entered the cell, with active extrusion by surface pumps and uptake into organelles. $I_{K(Ca)}$ decays somewhat faster than $I_{NS(Ca)}$ after a depolariza-

Address reprint requests to Dr. Robert S. Zucker, Physiology-Anatomy Department, University of California, Berkeley, CA 94720.

J. GEN. PHYSIOL. © The Rockefeller University Press · 0022-1295/89/06/1017/44 $2.00
Volume 93 June 1989 1017–1060

tion, because of its voltage-dependent relaxation combined with the decay of submembrane calcium. The interplay of these two currents accounts for the calcium-dependent outward–inward tail current sequence after a depolarization, and the corresponding afterpotentials after a burst of spikes.

INTRODUCTION

Changes in intracellular calcium concentration mediate many cell functions. Among these are the regulation of three calcium-dependent membrane currents which interact to control impulse activity in endogenously bursting pacemaker neurons in the left abdominal hemiganglion of *Aplysia* (Kramer and Zucker, 1985*a*, *b*): (*a*) A slow outward current, consisting of calcium-activated potassium current, $I_{K(Ca)}$, declines to 20% in ~500 ms after a depolarizing pulse. This is the dominant current for ~50 ms. (*b*) A slower inward current, consisting of calcium-activated nonspecific cation current, $I_{NS(Ca)}$, declines to 20% in ~1 s after a depolarization. (*c*) A late outward current arises from calcium-dependent inactivation of the calcium pacemaker current and lasts ~10 s after a depolarization.

Repetitive bursting activity is generated by the interplay of these three currents (Adams, 1985; Adams and Levitan, 1985; Kramer and Zucker, 1985*a*, *b*). Bursts are initiated by the weak pacemaker calcium current (Gorman et al., 1982), which is activated at potentials near rest. This current gradually depolarizes the neuron until threshold is reached and a burst of spikes is initiated. Each spike is followed by a hyperpolarizing afterpotential, due largely to the first slow outward current, $I_{K(Ca)}$. Calcium entering during spikes also activates the slow inward current or $I_{NS(Ca)}$, which helps to boost the burst by generating depolarizing afterpotentials that trigger successive spikes (Thompson and Smith, 1976; Smith and Thompson, 1987). Finally, accumulating intracellular calcium gradually blocks the pacemaker current by calcium-dependent inactivation (Eckert and Chad, 1984), terminating the burst with a long-lasting interburst hyperpolarization.

The roles played by these calcium-dependent currents depend critically upon their timing and duration. It has remained a puzzle why three membrane currents, all dependent on submembrane calcium activity during and after a burst, should decay at such different rates. We previously proposed that the receptors for calcium associated with these currents have different sensitivities to intracellular calcium, or that calcium exhibits different degrees of cooperativity in binding to the receptors and activating (or blocking) the respective currents (Kramer and Zucker, 1985*b*). A critical test of these ideas is one goal of this study.

A variety of techniques may be used to elevate intracellular calcium and activate calcium-dependent currents. However, only one, the release of "caged calcium" from photolabile chelators such as the nitr compounds (Adams et al., 1988), permits the quantitative control of calcium over a wide range at different times in an experiment on a single cell (Tsien and Zucker, 1986). Upon photolysis by ultraviolet radiation, nitr-5 and nitr-7 release calcium with time constants of 0.3 and 1.8 ms, respectively, and form only water as a byproduct. When a known mixture of calcium and nitr is injected into a neuron and exposed to a light flash of known intensity, the calcium concentration change at the front surface of the cell, facing the light

source, as well as the average calcium concentration in the cell as a whole, may be calculated.

We began this study with extensive calibration and testing of the behavior of nitr in vitro and in bursting neurons, to explore its properties when subjected to successive light flashes of different intensity. In the process, we developed programs for predicting free calcium concentration changes at the cell surface and in the interior after diffusional equilibration to a series of flashes. We extended this analysis to calculate the spatial distribution of free calcium release in a cell by a flash of light and the time course of its subsequent decay due to diffusion. We have confirmed several of these predictions in experiments combining nitr with the calcium-indicator dye, arsenazo III. We hope this exploration of nitr's properties, together with our models and tests, will serve as a general guide to the quantitative use of photolabile chelators of "caged compounds" as applied to problems in cell physiology.

We have used nitr to measure the calcium sensitivities and calcium activation stoichiometries of two of the currents involved in burst generation, $I_{K(Ca)}$ and $I_{NS(Ca)}$. To our surprise, we found that both these currents are activated by similar rises in intracellular calcium, and both with a cooperativity of one. Thus we are forced to reject our original hypothesis regarding the basis of the different decay rates of $I_{K(Ca)}$ and $I_{NS(Ca)}$. Our next step was to study the kinetics of $I_{K(Ca)}$ and $I_{NS(Ca)}$ when elicited by nitr photolysis. We found that diffusional equilibration of the calcium and nitr after a flash is the dominant determinant of the response decay rate. Surface calcium pumps also influence this time course. Although we cannot deduce stoichiometry of calcium action directly from the time course, the similarity of decay rates for the two currents when activated by nitr photolysis confirmed that the calcium stoichiometries are similar. We found that the key difference between $I_{K(Ca)}$ and $I_{NS(Ca)}$ is in their voltage dependences. After a depolarizing pulse or burst of spikes, a voltage-dependent relaxation of $I_{K(Ca)}$ speeds its decay relative to that of $I_{NS(Ca)}$. The conductance underlying the latter current is voltage independent and simply tracks the decline of submembrane calcium activity. The different time courses of these currents are well predicted from simple kinetic models and measurements of their voltage and calcium dependences.

METHODS

Computer Simulations

To use nitr as a quantitative tool in controlling intracellular calcium activity, we had to construct a model of nitr reactions and test its predictions. Computer simulations of the reactions of nitr with calcium and the effects of ultraviolet light were performed on a 12-MHz computer (model 286 AT; PC's Ltd., Austin, TX), using programs written in Quick Basic 2.0 (Microsoft, Redmond, WA). Simulations ran slower when patches (Micro Way, Kingston, MA) for the 80287-6 math coprocessor were installed, probably because access time to this chip obviated savings in computation time. Similarly, Quick Basic 3.0 with math coprocessor implementation also slowed computation speed. Therefore, routines using the math coprocessor were abandoned for our computations. On-line graphical displays of simulations were produced on a monitor (Multisync; Nippon Electric Corp., Wood Dale, IL) using Basic graphics statements, and hard copy was generated on a printer (model FX-80; Epson, Tor-

rance, CA) using a screen dump facility (Frieze; Z-Soft, Marietta, GA). Final graphics copy was produced with the Grapher program (Golden Software, Golden, CO).

In Vitro Measurements

To confirm the predictions of simulations of nitr chemistry, we used arsenazo III (Sigma Chemical Co., St. Louis, MO) to detect the calcium released by photolysis of nitr-5. To mimic as closely as possible the intracellular ionic environment, 250 μM arsenazo III and 10 mM nitr-5 (Calbiochem-Behring Corp., La Jolla, CA) were dissolved in a buffer consisting of 250 mM KCl, 50 mM NaCl, 3 mM $MgCl_2$, and 25 mM K-HEPES buffer (Sigma Chemical Co.), pH 7.5. This solution was drawn into a 5-mm length of No. 3530 Microslide, (Vitro Dynamics, Rockaway, NJ), having a nominal 300-μm path length. The microcuvette was kept under a layer of light mineral oil in a 35-mm plastic Petri dish inserted in the light path of our microspectrophotometer. Since the incident light was aimed at the cuvette from an angle of 30° from perpendicular, the path length through the tube was 346 μm.

Quantitative control of calcium concentration requires mixing nitr and calcium in precise amounts. We routinely checked our loading of nitr with calcium by measuring absorbance spectra on dilutions of our nitr mixtures before and after adding excess EGTA or calcium. The measured percent loading was often 10% higher than calculated, probably due to <100% purity of our nitr samples. We used the measured values of calcium loading in our predictions of effects of nitr in experiments.

Spectrophotometer

The spectrophotometer uses a focused beam of light from a 100-W quartz iodide lamp passed through one of four 10-nm band-width filters (Ditric Optics, Marlboro, MA) spun in a rotating wheel that completes one revolution every 20 ms. The filters are positioned at 60° and 120° and at 240° and 300°. The 0° and 180° positions are used by the spectrophotometer to sample the ambient light intensity. The colored light pulses, at 577, 610, 660, and 700 nm, were focused as a 100 μm diam spot onto the microslide using a f/1.4 lens, 25-mm focal length, and the transmitted light collected with a 1/16-in fiber optic clad rode (American Optical, Southbridge, MA) pulled to a tapered tip diameter of 150 μm. This arrangement minimizes stray light interference (Zucker, 1982). The tapered portion was covered with silver paint to prevent light loss or stray light acceptance, and coated with Isonel 31 Insulating Varnish (Schenectady Chemicals, Schenectady, NY). Incident light was collected with another clad rod near the bottom of the Petri dish containing the experimental specimen.

Incident and transmitted light were sensed with UV-100 photodiodes (EG & G, Electro-Optics Div., Salem, MA). After amplification, the light pulses were corrected for ambient light fluctuations by subtracting a signal proportional to the ambient light sampled by the photodiodes during the dark phases of the spinning wheel rotation. The incidence light pulses were used to control a demultiplexer circuit to separate the four wavelength signals of incident and transmitted light. Each incident light pulse was integrated until reaching a criterion level, and transmitted light for the same pulse was also integrated for this same period. This serves to standardize the amount of light in each incident light pulse, and automatically normalizes the transmitted light signal at each wavelength to a constant incident light intensity. It is thus equivalent to normal ratiometric spectrophotometry, but avoids actually performing a division of light signals. It also automatically corrects for fluctuations in incident light intensity due to light source and optical path noise. Gain equalizer circuits were used to adjust the transmitted light intensity to a uniform level after inserting the specimen, so that a 1% change in transmitted light intensity corresponds to 1 V. The spectrophotometer provides signals for transmittance at each wavelength, as well as two difference outputs, each corresponding to the differences between any two selected wavelengths. The maximum calcium

sensitivity of arsenazo III occurs at 660 nm, and subtracting 700 nm (the nearest calcium-insensitive wavelength) reduces noise due to specimen movements and osmotic changes, broad-band nonspecific absorbance changes in the specimen, and photodiode noise.

Flashlamp

Nitr photolysis was accomplished using a Strobex Power Pack (Chadwick-Helmuth, El Monte, CA) and 75-W xenon arc lamp. This instrument stores up to 230 J of electrical energy on capacitors which are discharged through the arc lamp when the xenon is ionized by a 12-kV pulse to a wire encircling the lamp. We modified the power pack to permit low level light flashes (down to 20 J) and rapid (7 s) recharging of the capacitor bank. To prevent lamp explosion, the discharge was prolonged using a Pulse Extender (Chadwick-Helmuth) which was wrapped in high-permeability metal foil (Co-Netic; Perfection Mica Co., Bensenville, IL) to minimize magnetic pulse interference with the electrophysiological gear. The light was focussed using an ellipsoidal ultraviolet-enhanced reflector (Melles Griot, Irvine, CA) with a 155-mm focal length. Infrared and short-wavelength ultraviolet radiation was removed using a 3-mm-thick liquid filter containing 1 M $Pr(ClO_4)_3$, 0.3 M $Co(ClO_4)_2$, and 0.25 M $Cu(ClO_4)_2$ between two quartz windows. This filter passed ultraviolet light between 300 nm and 430 nm at 70% transmittance, and visible light from 350 nm to 700 nm at about 20–50% transmittance.

This flashlamp produced flashes with a duration of about 400 μs. The flashlamp was calibrated in terms of its effectiveness in photolysing Ca-bound nitr-5 according to the procedure described in Tsien and Zucker (1986). This procedure makes no reference to the absolute quantum efficiencies of nitr-5, since these are difficult to measure accurately (cf. Tsien and Zucker, 1986; Adams et al., 1988). A 200-J flash protolyzed 35% of nitr-5 in excess calcium, corresponding to ~250 mJ/cm^2 of light energy at 340–370 nm, the waveband maximally effective at photolyzing nitr-5. From the relative quantum efficiencies of nitr-5 and nitr-7 (Adams et al., 1988), a 200-J flash also photolyzes about one-third of Ca-bound nitr-7, and ~12% of the free form of nitr-5 or nitr-7 in the absence of calcium.

To control for variations in flash intensity, we routinely sampled the incident light with a photodiode and amplifier, and recorded signals proportional to the light intensity during all experiments. We integrated the light signal, and expressed flash intensity as the fraction of light energy delivered by a 200-J flash. Thus, a flash with half the light energy was called a 100-J flash. This was, in fact, obtained by discharging close to 100 J through the flash lamp.

In order to use the flashlamp simultaneously with the spectrophotometer, we had to time flashes to occur during a dark phase of the four-wavelength light cycle. The light flash and its effects on the spectrophotometer were sufficiently brief that the transmittance signal recovered completely within one light cycle (20 ms).

Electrophysiological Experiments

Abdominal ganglia were removed from *Aplysia californica* specimens injected with 50 ml of 400 mM $MgCl_2$ as a relaxant. We desheathed ganglia in artificial seawater (495 mM NaCl, 10 mM KCl, 10 mM $CaCl_2$, 50 mM $MgCl_2$, 10 mM Na-HEPES, pH 7.5) made hyperosmotic by addition of 400 mM sucrose to shrink neurons away from the sheath. Experiments were performed on intact bursting pace-maker neurons from the dorsal left upper quadrant. We found it difficult to keep axotomized neurons healthy for the duration of these experiments. Since axon spikes may contribute to slow inward tail currents in bursting neurons (Adams and Levitan, 1985), it was important to block voltage-dependent sodium currents with 50 μM tetrodotoxin (Calbiochem-Behring Corp). Neurons were pressure injected with beveled microelectrodes, having a 1-μm opening, 2-μm outside diameter at the base of the bevel, and

a sharp (0.2-μm) tip, filled with 100–200 mM nitr-5 or nitr-7, loaded with $CaCl_2$ at 50–90% the nitr concentration. In many experiments, the electrode also contained 250 μM arsenazo III, and the absorbance of the neuron at 577 nm was monitored during injection. In this fashion we could determine the final arsenazo concentration, and also the final nitr concentration in injected cells. Injected neurons were viewed in light filtered to remove wavelengths below 450 nm to prevent nitr photolysis. Experiments were conducted at 18°C, using a Peltier effect cooler. Solution changes were accomplished with miniature valves (General Valve, Fairfield, NJ) placed near the ganglion, and with the inflow tube precooled to minimize temperature jolts. Silver wires or pellets in electrode holders and agar ground bridges were shielded from the light flashes to prevent photochemical artifacts. Membrane currents were recorded under voltage clamp from left upper quadrant pacemaker neurons on the dorsal surface of abdominal ganglia of *Aplysia californica*. Low-level membrane currents were recorded under voltage clamp and were usually filtered at 16 Hz to reduce noise. Our two-electrode voltage-clamp procedures and equipment, sample-and-hold circuit to subtract holding current at potentials far from rest, pressure injection procedure, and data recording and storage equipment are described elsewhere (Kramer and Zucker, 1985*a*; Tsien and Zucker, 1986).

Neurons filled with nitr and exposed to ultraviolet light flashes respond with increases in two membrane currents, a calcium-dependent potassium current, $I_{K(Ca)}$, and a calcium-dependent nonspecific cation current, $I_{NS(Ca)}$. Normally, these currents were elicited simultaneously as a mixed current (Tsien and Zucker, 1986). We separated these currents in one of three ways: (*a*) $I_{K(Ca)}$ could be isolated by clamping a neuron to the reversal potential of $I_{NS(Ca)}$ (−22 mV, Kramer and Zucker, 1985*b*), and $I_{NS(Ca)}$ could be isolated by clamping to the potassium reversal potential (−75 mV, Brown and Kunze, 1974). (*b*) $I_{NS(Ca)}$ could be recorded in isolation by selectively blocking $I_{K(Ca)}$ with 50 mM tetraethylammonium chloride (TEA), as reported by Hermann and Gorman (1981). We found that TEA had no effect on $I_{NS(Ca)}$ recorded at −75 mV. (*c*) $I_{K(Ca)}$ could be isolated by reducing $I_{NS(Ca)}$ by substituting tetramethylammonium (TMA) isosmotically for sodium (Zucker and Smith, 1979) and cobalt isotonically for calcium (Kramer and Zucker, 1985*a*).

RESULTS

Neural Responses to a Sequence of Flashes

Our chief goal was to measure the dependence of two membrane currents, $I_{K(Ca)}$ and $I_{NS(Ca)}$, on intracellular calcium activity by releasing calcium from nitr injected into single neurons on exposure to intense light flashes. We expected responses to identical flashes to be similar, except for a gradual decline due to exhaustion of the high-affinity nitrobenzhydrol form of nitr (Tsien and Zucker, 1986). However, in 23 experiments, this expectation was not borne out. Instead, we observed that successive flashes elicited increasing membrane currents for the first 2–10 flashes, with only later responses declining as expected (Fig. 1). We have therefore considered carefully the reactions of nitr with calcium and light, to better understand its behavior in neurons.

Computer Model of Nitr Responses

We describe in the Appendix the structure and rationale for a model (Model 1) which we developed to simulate nitr reactions in neurons. This model predicts the effects of successive light flashes on the surface and average cytoplasmic free cal-

cium concentrations in a neuron. To use the computer program implementing the model, only the flash intensity, cell diameter (needed to calculate average light intensity), concentrations of injected nitr and calcium, pump rate for calcium extrusion, and intervals between flashes (needed to calculate pump effects) need be entered. All parameters except pump rate are known. The pump rate is estimated by waiting a significant interval between flashes (e.g., 30–60 min) late in an experiment such as that illustrated in Fig. 1, when successive responses every 2 min are nearly constant, observing the drop in response amplitude after this interval, and choosing a pump rate to fit this drop.

In Vitro Tests of the Model

Before using this model to analyze physiological data, we tested its validity by comparing its predictions to actual measurements of calcium concentration changes. To

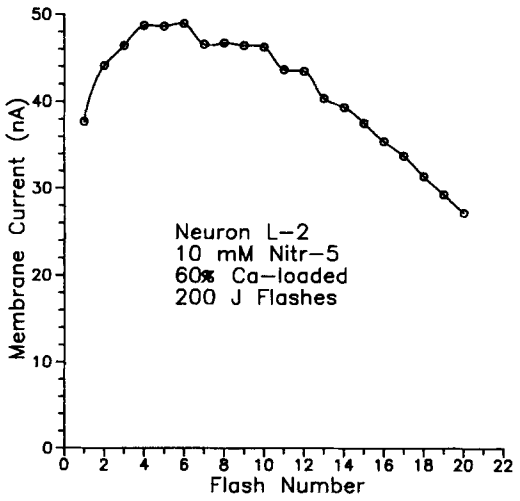

FIGURE 1. Successive peak increments in $I_{K(Ca)}$ recorded in neuron L-2 filled with 10 mM nitr-5 plus 6 mM $CaCl_2$ and exposed to 20 200-J flashes at one flash every 2 min. The cell was clamped at −20 mV to eliminate $I_{NS(Ca)}$.

do this, we used arsenazo III as a detector of changes in calcium concentration. We measured the absorbance change at the 660–700-nm wavelength pair of 250 μM arsenazo III mixed with 5–15 mM nitr and various amounts of added calcium, dissolved in a cytoplasm-resembling buffer in a microcuvette with path length similar to that of our neurons. We compared these observations with predictions of changes in average calcium concentration in the cuvette derived from our Model 1. For these simulations, a rectilinear geometry was used to calculate average light intensity in the cuvette (see Appendix), and the extrusion pump was omitted.

Before pursuing these experiments, we performed the following controls: (*a*) Solutions of arsenazo III without nitr showed no change in transmittance at the calcium-sensitive wavelengths when exposed to 200-J flashes from our flashlamp. (*b*) Solutions of nitr-5 without arsenazo III did show small broad-band transmittance changes in the visual spectrum upon exposure to bright flashes. These signals were cancelled by using the 660–700-nm wavelength pair, and therefore did not interfere with our measurement of calcium-sensitive arsenazo III transmittance changes.

The dependence of arsenazo III absorbance on calcium concentration in our buffer solution is plotted on conventional logarithmic axes in Fig. 2 *A*. The line represents a first-order reaction scheme fitted to the data points. One complication of the use of arsenazo III is that its responses begin to saturate at calcium concentrations of 10 μM. Since successive flashes may raise the calcium concentration to this or higher levels, saturation of arsenazo III must be taken into account. This is not so easily done, because we normally record the increment in light transmittance caused by a given flash. As the cumulative calcium concentration rises after successive flashes, arsenazo III becomes progressively more saturated, and the correspondence between increments in calcium concentration and increments in light transmittance changes, as seen from the linear plot of arsenazo III absorbance vs. calcium concentration in Fig. 2 *B*. Thus a given calcium concentration change will elicit

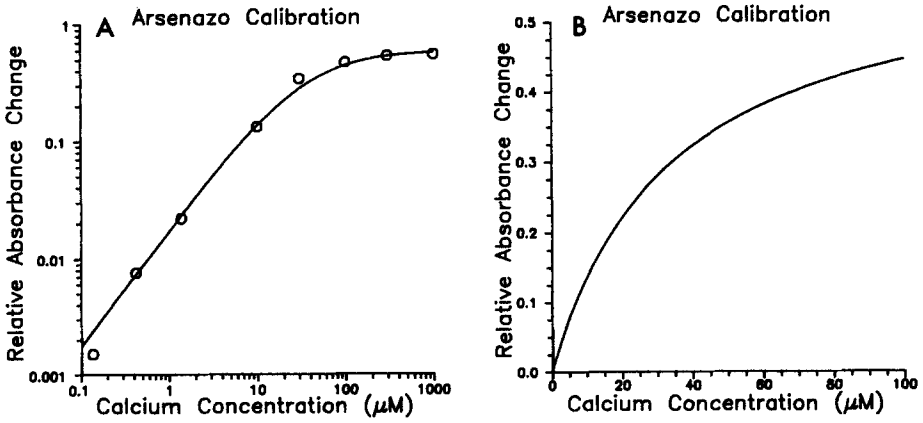

FIGURE 2. Calibration of arsenazo III in marine cytoplasm-like buffer. The ordinate plots the relative absorbance change at 660 nm relative to the absorbance of arsenazo III at its isosbestic point, 577 nm. This ratio is independent of path length. Calibration points are from Smith and Zucker (1980). The data are fitted to the curve relative absorbance change = 0.6 [Ca]/ ([Ca] + K), where K = 34.29 μM. This curve is plotted on logarithmic coordinates in *A*, and linear coordinates in *B*.

smaller and smaller arsenazo III absorbance changes as the calcium concentration rises and arsenazo III becomes saturated.

Fig. 3 illustrates the effect of this situation on changes in light transmittance accompaning a sequence of flashes. The solid lines in this figure represent the predicted effects of 15 flashes on the free calcium accumulation in a microcuvette. The dashed line shows how arsenazo III transmittance changes progressively fall behind the calcium concentration changes as dye saturation proceeds. Because there is no constant factor relating arsenazo III transmittance changes to calcium concentration changes in an experiment with many flashes, calcium concentration changes cannot be related linearly to observed transmittance changes.

To convert transmittance data to calcium concentration changes requires knowledge of the accumulated calcium level, but this is not measured experimentally. Therefore, it is improper to transform our transmittance data to calcium concentra-

tion changes for comparison to model predictions, because this transformation itself would be a model prediction. Instead, we have transformed our model predictions of calcium concentration changes to predictions of arsenazo transmittance changes, using the calibration curve of Fig. 2. Multiplying the ordinate of Fig. 2 by the absorbance of arsenazo in the cuvette at 577 nm yields the absorbance change at 660 nm (A) corresponding to a calcium concentration change. This is converted to percent transmittance change, T, by the formula $T = 10^A - 1$. These model predictions are compared directly to our measurements of successive transmittance change.

Fig. 3 also shows that our model predicts that the successive calcium concentration changes and arsenazo III transmittance changes should rise for the first few

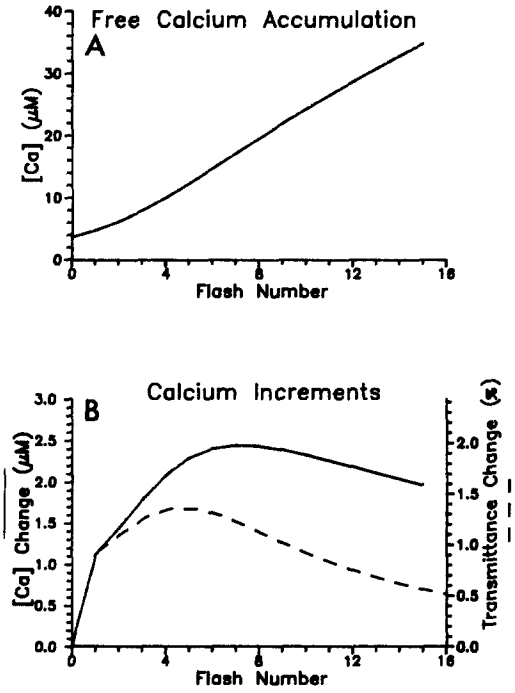

FIGURE 3. (*A*) Free calcium accumulation and (*B, solid line*) calcium concentration increments to 15 200-J flashes, calculated from Model 1 outlined in the Appendix. This simulation is for microcuvettes filled with 15 mM nitr-5 and 12.75 mM Ca. The dashed line in *B* shows the predicted transmittance change for 250 μM arsenazo in buffer medium, obtained from the calibration curve in Fig. 2. Note that in *B*, the starting $[Ca^{2+}]$ is 4 μM.

flashes, and then begin to drop. This is similar to the behavior of the calcium-dependent membrane currents observed in neurons (Fig. 1), which we initially found so puzzling. Looking carefully at what happens during successive flashes, we arrive at the following explanation: We start with 15 mM of nitr-5, 85% bound to calcium in Fig. 3. The first flash photolyzes 0.9 mM of the nitrobenzhydrol to nitrosobenzophenone, leaving 14.31 mM of the benzhydrol, which is now 88% bound to calcium. This flash releases 0.14 mM calcium onto the nitrosobenzophenone. The next flash photolyzes 0.61 mM of the nitrobenzhydrol, leaving the high-affinity buffer 91% loaded with calcium, and releasing 0.19 mM calcium onto the nitrosobenzophenone. Each flash leaves less of the high-affinity buffer, without changing the total calcium concentration, so that the buffer is progressively more saturated.

Consequently, photolysis of the remaining buffer releases larger and larger amounts of calcium onto the nitrosobenzophenone that is being formed. Meanwhile, the nitrobenzhydrol is being progressively reduced, so that successive flashes photolyze less and less nitrobenzhydrol. Moreover, as the more absorbent nitrosobenzophenone is formed, the average effective flash intensity is diminishing. Eventually, the latter effects overtake the effect of nitrobenzyhdrol saturation, at which point the peak calcium concentration change occurs. Subsequent flashes release less calcium onto the low-affinity nitrosobenzophenone. As Fig. 3 *B* shows, arsenazo III saturation may cause the transmittance changes to reach a peak before the calcium concentration changes do.

Fig. 4 illustrates the expected effects of varying different solution and flash parameters. Flashes were repeated at 2-min intervals. Since the spectrophotometer light path crosses from the front to the rear of the microcuvette, it records a roughly average calcium concentration change in the cuvette. Because of arsenazo's saturation, spatial averaging of arsenazo signals is not strictly legitimate. We often observed a small increase in arsenazo absorbance during the first few seconds after a flash. This may reflect the diffusion of calcium and desaturation of arsenazo at the top of the cuvette. For this reason, we measured the steady absorbance change 20–30 s after each light flash.

Fig. 4 *A* shows that if the nitr is initially more heavily loaded, nitrobenzhydrol exhaustion overtakes nitrobenzhydrol saturation sooner, and the peak calcium concentration change occurs sooner. Also, the heavily loaded nitr initially releases much larger calcium increments onto the low-affinity buffer. The predicted arsenazo III transmittance changes are generally close to those observed experimentally under the modeled conditions. Experiments with more highly loaded nitr-5 are more susceptible to errors in making calcium-nitr mixtures, imperfect knowledge of calcium-nitr-5 affinities, imperfect measurement of specific absorbance of nitr-5 forms, etc. Thus experimental data deviate more from model predictions as loading increases.

Fig. 4 *B* shows the effect of varying nitr concentration at constant calcium loading. Cuvettes with higher nitr concentrations absorb more light, so that the average flash intensity is reduced. This is equivalent to reducing flash intensity, and results in less average nitr photolysis, smaller calcium concentration changes, and arsenazo III transmittance changes, and more flashes before reaching the peak response. Again, the model predictions match closely the experimental results obtained with different nitr concentrations.

Fig. 4 *C* shows the effect of varying flash intensity on successive flash responses. Brighter flashes photolyze more nitr, leading to larger responses and an earlier peak. Data are shown for 100- and 200-J flashes, and they match the predictions reasonably well. We also show the predicted effects of a 10% increase or decrease in the intensity of the flashes from 200 J. This reflects the precision of the flashlamp or of the photodiode detector, in that responses of the photodiode to flashes set to the same nominal intensity fluctuate within this range. This provides an indication of the precision with which we can control the photolysis of nitr with our apparatus, and the magnitude of difference between model prediction and experimental observation which we must be prepared to tolerate.

Fig. 4 *D* shows the effect of five flashes of increasing intensity on the arsenazo III

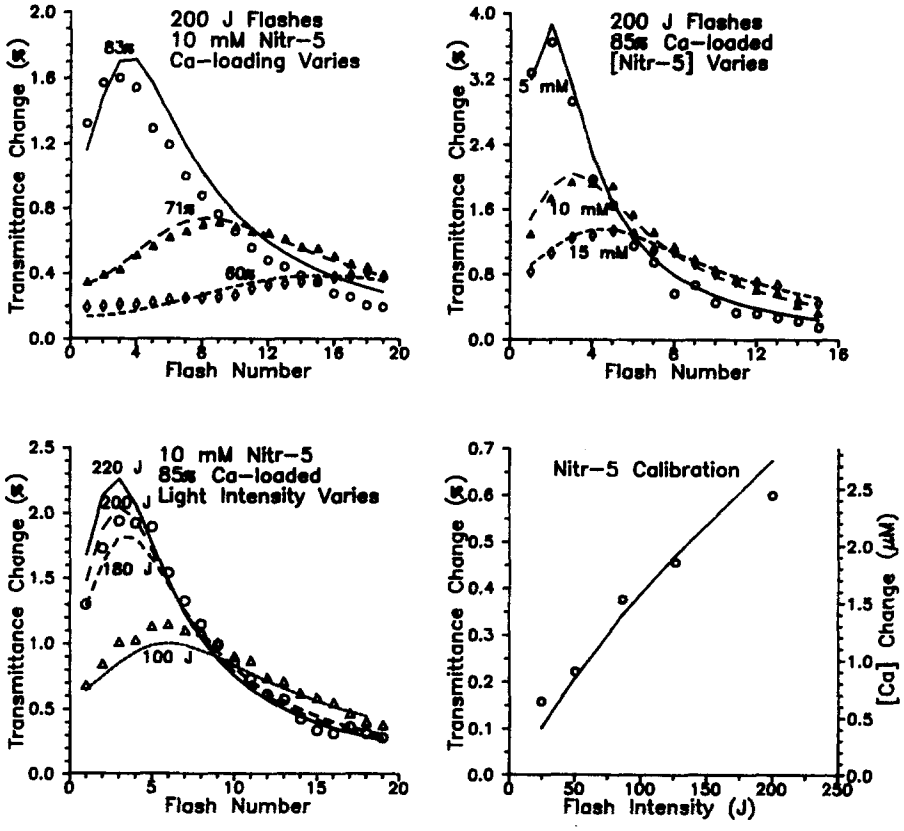

FIGURE 4. Model predictions of changes in calcium concentration expressed as arsenazo III transmittance changes (*lines*), compared to in vitro experimental observations (*symbols*). (*A*) The microcuvette was filled with 10 mM nitr-5 loaded with calcium to either 60%, 71%, or 83% as indicated and exposed to 200-J flashes. (*B*) Microcuvettes were filled with either 5, 10, or 15 mM nitr-5 as indicated. The nitr was 85% loaded with calcium and exposed to 200-J flashes. (*C*) 10 mM nitr-5 and 8.5 mM calcium was exposed to trains of either 100 or 200 J. Predictions of responses to 180- and 220-J flashes are also shown to indicate the effects of light flash variability within the level of accuracy of the apparatus. (*A–C*) A 1% transmittance change corresponds to a $\Delta[Ca^{2+}]$ of 1.2 μM. (*D*) Responses to flashes increasing in intensity from 24 to 200 J are shown. The cuvette contained 10 mM nitr-5 and 8.5 mM calcium, and had been exposed to 14 flashes at 125 J. The transmittance changes are converted to calcium concentration changes as explained in the text to produce this nitr calibration curve. All cuvettes contained 250 μM arsenazo III in buffer ionically similar to marine cytoplasm.

transmittance changes. We preceded these flashes with 14 flashes at 125 J to move past the peak of nitr responses and into a region of reasonably constant responses to repeated identical flashes. We proceeded from weak to strong flashes to minimize the effect of prior flashes within the sequence, so that all flashes act on a roughly constant mixture of nitrobenzhydrol and nitrosobenzophenone. The line plots predicted results, and the symbols show experimental observations.

The experiment of Fig. 4 *D* was performed at a starting calcium concentration of

31 μM (due to prior partial nitr-5 photolysis). If we convert transmittance changes to absorbance changes, and divide by the absorbance of arsenazo at 577 nm, we can convert to calcium concentration changes using the slope of Fig. 2 *B* at 31 μM. This is shown as the right-hand ordinate of Fig. 4 *D*. This "calibration curve," relating flash intensity to calcium concentration change, is applicable only to the nitr concentration (10 mM), initial percent loading (85%), and history of light flashes and nitr photolysis (14 125-J flashes, 37.8% nitr photolyzed) of this particular experiment.

In Vivo Tests of the Model

The above results gave us some confidence that we could predict the effect of flash photolysis of nitr-5 on the calcium concentration in microcuvettes. Additional experiments indicate that our model also predicts correctly the calcium concentration changes in neurons filled with nitr compounds. Fig. 5 shows the transmittance changes observed in three neurons filled with nitr-5 and arsenazo III. For all cells, we show the transmittance change at the wavelength pair (660–700 nm), which is maximally sensitive to calcium. In Fig. 5, *B* and *C*, we also show transmittance signals at 610–700 nm. As expected for a calcium concentration change (Smith and Zucker, 1980), the arsenazo III signal at 610 nm was roughly half that at 660 nm. A change in pH or magnesium concentration, or an artifact due to cell movement or osmotic changes, would have caused transmittance changes at 610 nm larger than or equal to those at 660 nm (Smith and Zucker, 1980; Zucker, 1981). In all three cells, we clamped the neuron to the reversal potential for $I_{NS(Ca)}$ to obtain a record of $I_{K(Ca)}$ in isolation, which is illustrated in Fig. 5 *C*.

For each cell, the dotted line shows the magnitude of the transmittance change predicted from our model. This prediction requires that we convert predicted calcium concentration change to transmittance change. To do this, we must know the arsenazo concentration in the cell. This was estimated from the absorbance change at 577 nm measured during filling of the neuron (Smith and Zucker, 1980). The correspondence between calcium concentration change and relative absorbance change was derived from the calibration curve of Fig. 2, corrected for deviations of the estimated arsenazo III concentration from 250 μM, as explained in Smith and Zucker (1980), and converted to 660-nm transmittance changes. In the three experiments illustrated in Fig. 5, average free calcium rose by 206, 379, and 210 nM in *A–C*, respectively.

In six experiments, the observed transmittance changes ranged from 62% to 150% of the predicted responses. Arsenazo III signals are highly dependent on the arsenazo III concentration, which is known only as well as the path length through the cell. We estimate this with an optical micrometer along an axis different from those followed by the photolysis light and the microspectrophotometer beam. The average light intensity in the cell, and consequently the proportion of nitr photolyzed by a flash, also depend critically upon the path length and the nitr concentration (see Appendix). Other sources of error include the accuracy of preparing small volumes (20–50 μl) of nitr-5 and calcium mixtures, and our estimate of the amount of injected calcium that has been extruded by pumps. Recognizing these errors, we regard the agreement between prediction and observation as satisfactory.

Calcium Dependence of $I_{K(Ca)}$

To estimate the degree of calcium cooperativity in activating membrane currents, we plot the peak amplitudes of currents evoked vs. the magnitude of the calcium concentration change caused by flashes of different amplitude. At the outset, we need to emphasize the importance of minimizing the resting calcium concentration. Let the resting calcium concentration be unity, and let ϵ represent an incremental

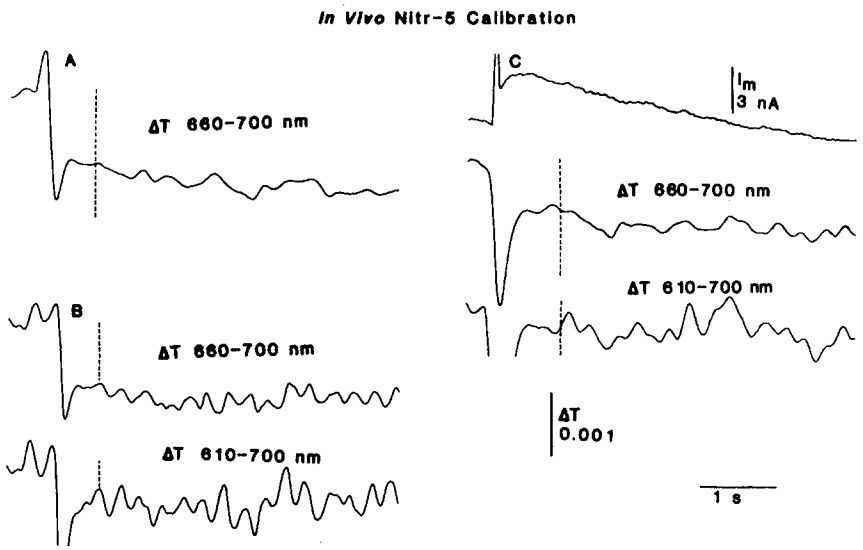

FIGURE 5. (*A–C*) Transmittance changes (*T*) from three different neurons injected with nitr-5 and arsenazo III. In each cell the transmittance change at the wavelength pair 660–700 nm is shown. In the cells of *B* and *C*, the transmittance change at 610–700 nm is also shown. In the last cell, the membrane current (I_m) of the neuron is also displayed, when the cell had been voltage-clamped to −24 mV. The dotted line shows the predicted transmittance change, calculated as explained in the text. (*A*) Responses to the first flash at 100 J; (*B*) responses to the third flash at 200 J; (*C*) traces are from the third flash at 100 J. Transmittance records are digitally smoothed with a 100-ms period in *A* and *B*, and a 250-ms period in *C*. The current in *C* was electronically filtered with a 10-ms time constant. The calculated nitr-5 and arsenazo concentrations are 10 mM and 250 μM in *A* and *B*, and 6.07 mM and 152 μM in *C*. Nitr-5 was injected with 75% bound to calcium and 25% free. The transmittance calibration bar of 0.001 corresponds to average cytoplasmic calcium concentration changes of 111 nM, 111 nM, and 203 nM in *A* to *C*. The cell diameters were estimated as 375, 350, and 500 μm in *A–C*.

rise in calcium concentration expressed as a fraction of the initial resting level. If a current is activated by n calcium ions acting simultaneously, then the incremental current accompanying the rise in calcium will be given by $\Delta I = (1 + \epsilon)^n - 1$. For $\epsilon \gg 1$, this reduces to ϵ^n, but for $\epsilon \ll 1$, this approaches $n\epsilon$. Thus any stoichiometry of calcium action will appear linear in the presence of a large initial calcium concentration.

The relevance of this effect may be appreciated by reference to Fig. 3, which shows that average calcium concentration increments are always less than the resting

calcium level. Fortunately, the situation for membrane currents is not so severe. These currents are activated by calcium concentration changes at the front surface of the cell which are much larger than the average changes. Fig. 6 shows model predictions of increments in a membrane current which depends on the third power of calcium concentration when a cell is exposed to six light flashes of increasing intensity. When plotted on double-logarithmic coordinates, predicted responses to the weak flashes fall on a line of unity slope, but larger flashes should elicit responses whose slope approximates that of the underlying cooperativity. From Fig. 3, we would expect that after several bright flashes, the resting level of calcium will have risen so high that it will exceed even the surface increments. Fig. 6 shows that after 10 200-J flashes, even the brightest flashes will elicit responses that barely

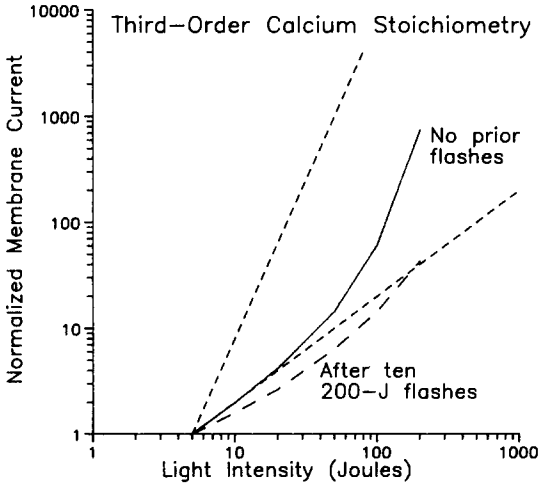

FIGURE 6. Effect of initial calcium concentration on the predicted relationship between amplitudes of calcium-dependent current and flash magnitude. It is assumed that the membrane current, e.g., $I_{K(Ca)}$, depends on the third power of calcium concentration. Predicted responses to a sequence of six light flashes (5, 10, 20, 50, 100, and 200 J) are shown when presented shortly after injecting a neuron with nitr-5 (*solid line*), and after 10 200-J flashes (*dashed line*). Responses are normalized to the effect of the weakest flash. A 200-J flash raises the surface calcium concentration 4.8 μM in the first flash sequence, and 3.7 μM in the second flash sequence. The accumulated average calcium level is 1.8 μM for the first flash sequence, and 4.0 μM for the second. The dotted lines represent slopes of 1 and 3. Calculations assume a 300-μm cell injected with 10 mM nitr-5 and 7.5 mM calcium. Flashes are repeated once per 2 min, and a pump time constant of 3 s in the absence of buffering (about 85 min in a cell filled with nitr) is assumed.

deviate from linearity. Therefore, it is essential when studying the calcium stoichiometry of membrane currents that a rising sequence of only a few flashes be used right at the beginning of the experiment.

Calcium-activated potassium currents from such an experiment are illustrated in Fig. 7. Light flashes of nominal energies of 10, 50, 100, and 200 J elicited the membrane current shown. When the actual light energy corresponding to each flash was measured with a photodiode and flash energies normalized to the brightest at 200 J, we arrived at flash intensities of 34, 82, 126, and 200 J. Our model predicted increments in surface calcium concentration of 0.11, 0.66, 1.52, and 3.54 μM.

Flashes evoked membrane currents whose peaks occurred shortly after the flash. The peak reflects the effect of the calcium concentration change at the surface of

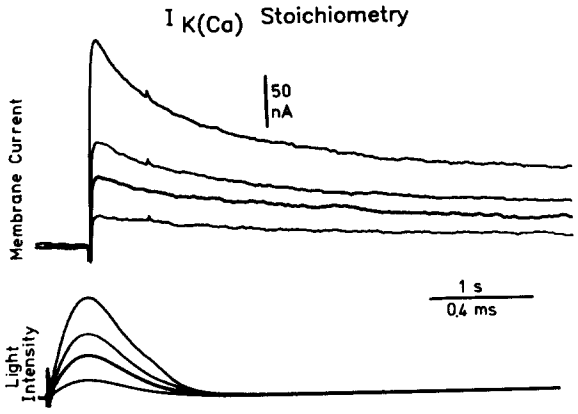

FIGURE 7. Calcium-activated potassium currents recorded from neuron L6 filled with 5 mM nitr-5 and 3.75 mM calcium. The bottom traces show the photodiode monitor of light intensities for four flashes. Increasing flashes were calculated to raise surface calcium concentration by 0.11, 0.66, 1.52, and 2.54 μM. The cell was voltage clamped to the reversal potential for $I_{NS(Ca)}$ (−22 mV) before each flash. The medium was normal artificial seawater containing 50 μM tetrodotoxin.

the neuron facing the light source. We show below that the subsequent decline in current is due to diffusion of released calcium away from the front surface. Therefore, it is peak membrane current which we relate to the calcium concentration change at the front surface of the cell. For a large cell filled with nitr-5, the calcium concentration at the back surface of the cell at the time of the flash is negligible (Tsien and Zucker, 1986).

The results from experiments on 17 upper left quadrant bursting neurons are plotted in Fig. 8. Included are cells in which $I_{NS(Ca)}$ was blocked by clamping the neuron to its reversal potential in normal saline (*open symbols*), and experiments in

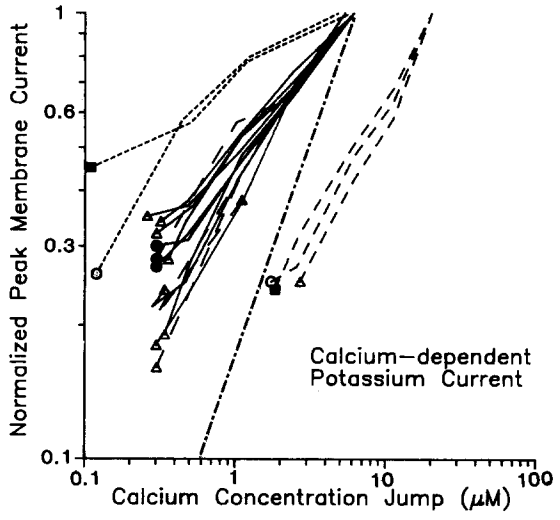

FIGURE 8. Relationship between peak $I_{K(Ca)}$ and calculated front-surface calcium concentration jump in 17 bursting pacemaker neurons. $I_{NS(Ca)}$ was blocked either by clamping the cell to its reversal potential (*open symbols*) or by removing sodium and calcium from the saline (*filled symbols*). The symbol marks the response to the first (usually weakest) flash in each cell. Neurons were injected with either 20 mM (*solid lines*) or 10 mM (*long dashed lines*) nitr-5 75% loaded with calcium, 20 mM nitr-5 90% loaded with calcium (*medium dashed lines*), or 20 mM nitr-7 75% loaded with calcium (*short dashed lines*). The membrane potential was held at −10 mV (*circles*), −20 mV (*triangles*), or −30 mV (*squares*). The current evoked by the brightest flash ranged from 3 to 122 nA in these neurons. The straight dot-dashed line has a slope of 1.

which $I_{NS(Ca)}$ was blocked in saline containing no sodium or calcium (*closed symbols*). For each data set, the symbol marks the first of typically five flashes. This flash was usually the weakest. In different cells, data were collected at potentials ranging from −10 to −30 mV (coded by the symbol type). The line type indicates the nitr solution injected. We filled most cells with either 10 or 20 mM nitr-5, 75% loaded with calcium. Three cells were filled with 20 mM nitr-5 plus 18 mM calcium (90% loaded), in order to explore responses to larger calcium concentration changes. Two neurons were injected with 20 mM nitr-7, 75% loaded with calcium, to obtain responses to smaller calcium increments.

The results are remarkably consistent. $I_{K(Ca)}$ amplitude was linearly related to calcium concentration change over a 200-fold range (100 nM to 20 μM jumps). In all experiments, the resting calcium concentration was about equal to the calcium increment of the flash of middle intensity. The brightest flash raised the calcium at the surface to between three and six times its prior level, so stoichiometries different from one should have been readily detectable.

The linear dependence of $I_{K(Ca)}$ upon calcium jump was observed at all membrane potentials between −10 and −30 mV. This suggests that only one calcium ion binds to the $I_{K(Ca)}$ channel at any voltage in this range.

The data show no clear tendency toward saturation. Therefore, even the largest calcium jumps used (20 μM, to peak levels of 26 μM with 90%-loaded nitr-5) apparently failed to exceed the affinity of calcium for the receptor responsible for activating $I_{K(Ca)}$. The data could not all be from a saturating region, because they span a response range of nearly a decade in each cell.

Calcium Dependence of $I_{NS(Ca)}$

We performed a similar study of the calcium stoichiometry of $I_{NS(Ca)}$. Fig. 9 shows results collected from eight neurons. As with $I_{K(Ca)}$, the conditions were varied to extend the range of calcium jumps to about a 100-fold range. Cells were injected with 10–20 mM nitr-5 75% loaded with calcium, or 10–20 mM nitr-5 90% loaded with nitr-5. We also injected some cells with 75%-loaded nitr-7, but the largest $I_{NS(Ca)}$ signals were <1 nA. With a noise level of ~0.2 nA, the data were regarded as too unreliable, so the results are not included in the figure.

As was the case with $I_{K(Ca)}$, $I_{NS(Ca)}$ depended linearly upon calcium concentration jump. These data also show no sign of saturation to calcium jumps of 20 μM to peak levels of 25 μM, or of dependence upon membrane potential, which was varied between −50 and −77 mV, the potassium equilibrium potential (Brown and Kunze, 1974). Thus it appears that both calcium-dependent membrane currents in *Aplysia* are activated linearly by similar levels of submembrane calcium activity.

Estimating Calcium Stoichiometry and Extrusion Rate from Sequential Responses

Our model for calculating calcium concentration changes in neurons includes a provision for a calcium sequestering or extruding system. The pump rate is a parameter of this model which must be chosen. We have estimated this parameter by exposing a neuron to a sequence of flashes until the responses are gradually declining. We then pause for ~30–60 min, and then resume flashing. Responses typically drop to about half in this time. By assuming a linear relationship between surface calcium

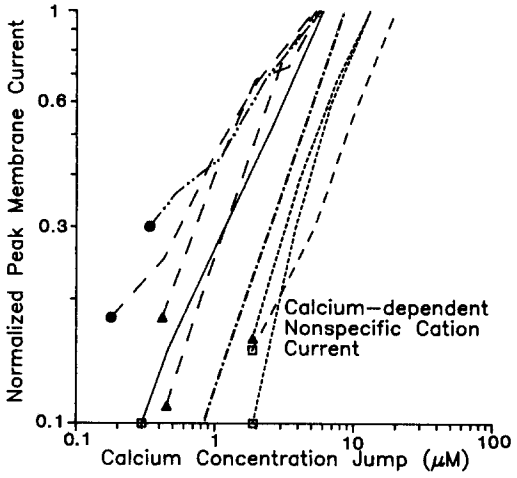

FIGURE 9. Relationship between peak $I_{NS(Ca)}$ and calculated front-surface calcium concentration jump in eight bursting pacemaker neurons. $I_{K(Ca)}$ was blocked either by clamping the neuron to the potassium equilibrium potential in normal artificial seawater (*open symbols*) or by addition of 50 mM TEA (*filled symbols*). The symbol marks the first flash in the sequence and indicates the membrane potential of the command signal as −50 mV (*circles*), −60 mV (*triangles*), or −77 mV (*squares*). Cells were injected with either 20 mM (*solid line*), 15 mM (*dot-dot-dashed line*), or 10 mM (*long dashed lines*) nitr-5 75% calcium-loaded, or with 20 mM (*medium dashed line*) or 10 mM (*short dashed lines*) nitr-5 90% calcium-loaded. The maximum response ranged from 0.5 to 8 nA in these cells. The straight dot-dashed line has a slope of 1.

increments and membrane current, we can vary the pump rate until the model simulations fit the results. In particular, we choose a pump rate such that the response after the pause is the same fraction of the predicted largest response as was observed experimentally. An example of such an experiment on $I_{K(Ca)}$ is shown in Fig. 10.

In this neuron, we obtain a reasonably good fit with a pump that removes unbuffered free calcium with a time constant of 3.5 s. Since 10 mM nitr-5 imposes a ratio

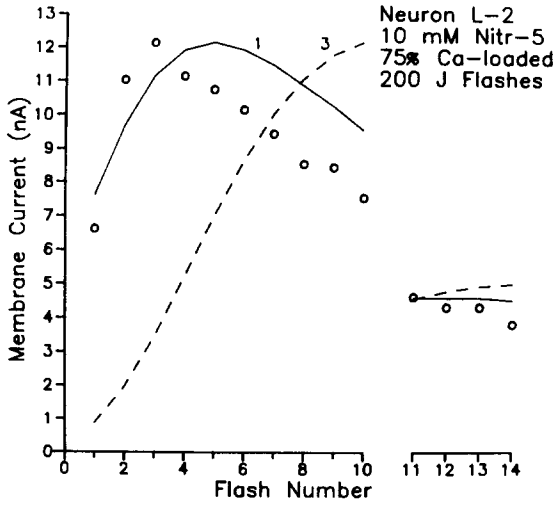

FIGURE 10. $I_{K(Ca)}$ recorded from neuron L2 injected with 10 mM nitr-5 and 7.5 mM calcium. 10 200-J flashes were issued at one per 2 min, and four more flashes were generated after a 25-min pause. The solid line is the predicted response in a cell with a calcium extrusion pump time constant of 3.5 s, assuming a linear dependence of $I_{K(Ca)}$ upon calcium concentration. The dashed line assumes a third-order dependence of $I_{K(Ca)}$ on calcium, and uses a pump time constant of 15 s.

of bound to free calcium of ~1,500, this corresponds to a calcium removal time constant of about 90 min. In this figure, we scale the predicted magnitude of membrane current to have the same peak as that observed experimentally.

A different result is obtained by assuming a higher stoichiometry of calcium action on $I_{K(Ca)}$. For example, a stoichiometry of 3 yields the prediction of the dashed line in Fig. 10. Again, the pump was adjusted so the first response after the pause was equal to the same fraction of the peak response as shown by the data. Since membrane current is assumed to be more sensitive to calcium concentration, a smaller drop in calcium is needed to cause the observed drop in response after the pause. This requires a slower pump rate, with a 15-s time constant.

Fig. 10 shows an additional interesting prediction. For a stoichiometry of 3, the model predicts that responses will continue to rise throughout the initial sequence of 10 flashes. The reason for this is as follows: although in both cases the surface calcium increments rise to a peak at the fifth response, the absolute level of calcium continues to rise. Thus, when the pump time constant is 15 s, the fifth flash causes the surface calcium to rise by 8.46 μM from 4.69 μM to 13.15 μM. By the tenth flash, calcium rises only 7.44 μM, but it starts at 9.16 μM and reaches 16.61 μM. If the cubed calcium concentration before the flash is subtracted from the cubed calcium concentration after the flash, it is readily seen that a smaller increment leads to a larger response in the tenth flash, when all calcium activities are higher. No such effect occurs for a linear stoichiometry.

The important result is that in 39 experiments, we never saw such behavior. Neither $I_{K(Ca)}$ nor $I_{NS(Ca)}$ responses continued to rise during a large number of successive flashes, as expected for a current nonlinearly dependent on calcium activity. Our results were always fit best by assuming a stoichiometry of unity.

Time Course of Membrane Currents Elicited by Calcium Released from Nitr

Our next objective was to understand the time course of membrane currents elicited by flash photolysis of nitr-5. Whether recording $I_{K(Ca)}$ or $I_{NS(Ca)}$, the typical response to a flash was a rapid rise to peak, followed by a gradual decline in response to half in 3–12 s, and approaching a steady-state level about one-third the peak (Figs. 7 and 13–15). Tsien and Zucker (1986) proposed that the response decay reflected primarily diffusion of calcium away from the surface facing the light, where the largest release occurs, as well as diffusion of the newly formed nitrosobenzophenone away from the front and its replacement by nitrobenzhydrol diffusing forward from the darker interior of the cell.

Computer Simulations of Flash Responses

To test this explanation, we expanded our model of nitrobenzhydrol photolysis and multiple buffer equilibration to include one-dimensional diffusion of all species that we expect to be present following a light flash, where we represent a cell as a cube. This model is described as Model 2 in the Appendix. Its parameters include the conversion efficiency of our flashlamp, calcium affinities of nitr and native buffers, extinction coefficients of all nitr species and cytoplasm, and diffusion constants of all species. All parameters have either been measured or may be estimated from published values, as described in the Appendix.

Predicted Responses to Light Flashes

Calcium-activated membrane currents depend only upon the submembrane calcium concentration. To predict such responses, we calculate the average surface calcium concentration in our cubic representation of a cell. We average the calcium at the front surface with the calcium on the sides of each slice of cytoplasm behind the surface, weighted according to its contribution to the cell surface (the slice thickness times the periphery). Since a real spherical cell tapers off toward the back (but the whole front surface is exposed to the incident light intensity), our procedure tends to overemphasize the contribution from hindmost shells. To compensate, we usually ignored any contribution from the back surface. Including or excluding the rear surface had very little effect on the form of the results, since the responses are dominated by changes in calcium at the surface facing the light source.

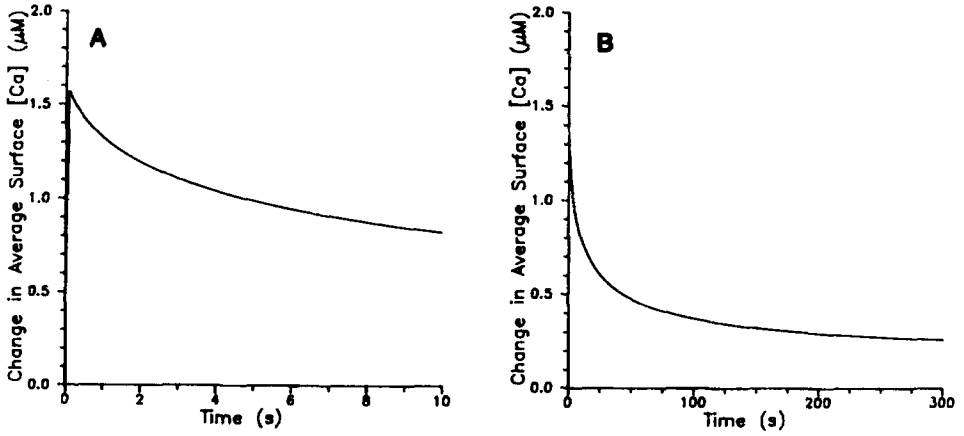

FIGURE 11. Predicted time course of change in free calcium concentration, averaged over the cell surface, plotted on (*A*) fast and (*B*) slow time scales. The peak in *B* is lower than *A* because the time bins in *B* were larger (50 ms) than in *A* (5 ms). The peak in *A* is accurate; that in *B* is affected by the decay which occurs within the first 50 ms. This simulation is for the fifth 200-J flash, repeated once per 2 min, in a 300 μm diam cell injected with 10 mM nitr-5 and 7.5 mM calcium.

Fig. 11 illustrates the predicted form of the flash response of a membrane current linearly dependent on intracellular calcium activity. Since the factor relating calcium concentration and membrane current is not known, we plot average subsurface concentration on fast and slow time bases. The simulated response drops to half in 10 s, and in 2 min it reaches 90% of its steady-state level, which is 20% of its peak. This simulation falls within our range of observed responses, suggesting that diffusion of calcium and nitr is primarily responsible for the decay of membrane currents following release of "caged calcium."

We questioned whether it is necessary to include diffusion of nitr and cytoplasmic buffer in our simulations. Ignoring diffusion of the native buffer has no discernible effect, because it is assumed to diffuse only very slowly, and it is overwhelmed by the nitr injected into the neuron. However, setting nitr diffusion constants to zero gen-

erates responses that decay very slowly, dropping only 15% in 10 s. We have never seen such slow responses, indicating that nitr is not strongly bound, but rather diffuses freely at about the rate expected for such a compound. Moreover, nitr diffusion is evidently an essential aspect of our model.

Factors That Affect the Decay of Responses

Calcium stoichiometry. We originally hoped to infer the stoichiometry of calcium action from the decay rate of flash responses. Certainly, a membrane current which depends on a high power of submembrane calcium will decay more rapidly than a current which depends linearly on that calcium concentration. Our simulations suggest that a current activated cooperatively by three calcium ions would decay to 17% of its peak in 10 s, while a linearly activated current would drop only to 39%. Unfortunately, this prediction was of little use in determining the stoichiometries of $I_{K(Ca)}$ and $I_{NS(Ca)}$, because in different experiments, either current could decay as slowly or as rapidly as our first- and third-order simulations. We therefore sought to find other factors that might influence decay rate.

Nitr concentration. The concentration of nitr in the neuron is one of these factors. In a heavily injected cell the average light intensity is much dimmer than if the nitr concentration is low, due to the absorbance of ultraviolet by nitr. The light intensity at the surface is the same, regardless of nitr concentration. Therefore, the first flash will convert 35% (per 200 J discharge energy) of the surface nitr, leading to a 3 μM increase in front surface calcium in the cell filled with 10 mM nitr-5 and a 4 μM increment in front surface calcium in the cell filled with 30 mM nitr-5, if nitr-5 is 75% loaded with calcium. The difference is due to the effect of the native buffer competing more with 10 mM nitr-5 than with 30 mM nitr-5. However, the light intensity will drop off faster with depth in the cell filled with the higher nitr concentration. Therefore, the volume-average calcium concentration change for the first flash will be 438 nM in the cell filled with 10 mM nitr, but only 213 nM in the cell filled with 30 mM nitr-5, due to the dimmer light intensity.

Fig. 12 illustrates spatial and temporal profiles in free calcium concentration caused by the fifth 200-J flash in two cells, where the only difference is in the amount of 75% Ca-loaded nitr-5 injected into the cells. The profiles of free calcium formed by the flash are different in the two cases. In the cell filled with 10 mM nitr-5, the calcium concentration at the moment of the flash drops to half its surface peak in ~25 μm, while in the cell filled with 30 mM nitr-5, the calcium drops to half only 12 μm behind the front surface. The sharper spatial gradient of calcium formed in the cell with 30 mM nitr leads directly to a more rapid diffusional equilibration of calcium in the cell. This may be seen as a more rapid drop in calcium at the front surface in the cell filled with 30 mM nitr. Similarly, the average surface calcium concentration drops faster in the cell filled with 30 mM nitr-5 (data not shown). Thus nitr concentration strongly influences the time course of membrane currents elicited by flash photolysis of nitr.

Calcium extrusion. The Na/Ca exchanger (Requena, 1983) also appears to affect the time course of flash-evoked current. Fig. 13 *A* shows results from one of four similar experiments. The curves marked "Na" are flash-evoked membrane currents in a neuron filled with nitr-5 and voltage clamped at −22 mV. This is the

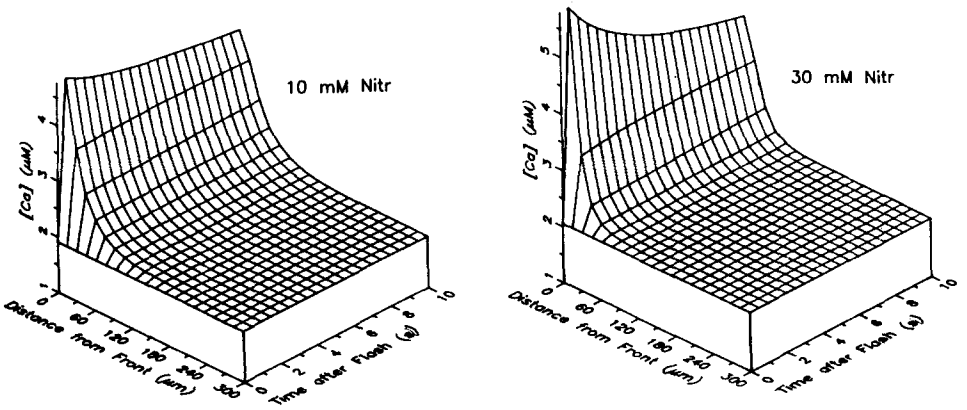

FIGURE 12. Predicted spatial and temporal profiles of intracellular free calcium concentration after the fifth 200-J flash at one per 2 min in 300-μm neurons filled with either 10 mM (*left*) or 30 mM (*right*) nitr-5 75% loaded with calcium. Each point is the calcium averaged over a 15-μm thick shell during a 500-ms time period. The initial peak calcium concentration change right at the surface is underestimated by this spatial smoothing.

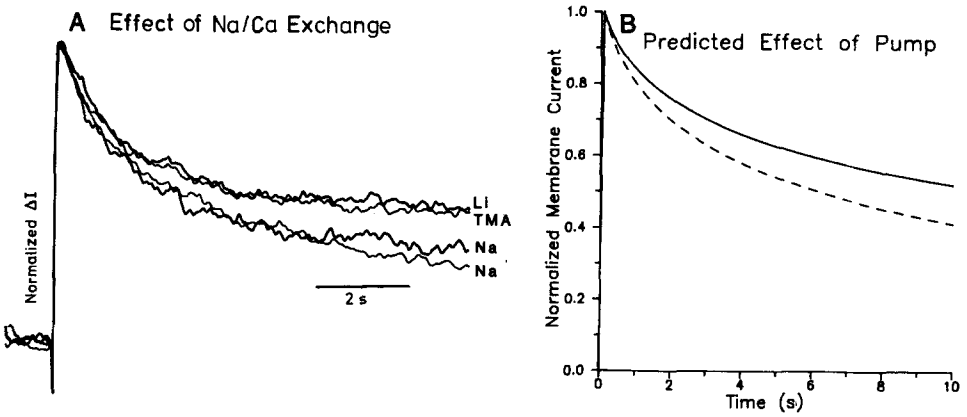

FIGURE 13. Effect of Na/Ca exchange on decay of flash-evoked $I_{K(Ca)}$. (*A*) Normalized responses to four 100-J flashes at −22 mV in a cell injected with 5 mM nitr-5 and 3.75 mM calcium. The upper trace marked "Na" was the response in normal seawater. The solution was changed to one containing TMA in place of Na, and the response marked "TMA" was obtained. Then the solution was changed to one with Li in place of Na, and the response marked "Li" was recorded. Finally, seawater was perfused through the bath, and the lower response marked "Na" was recorded. The upper two traces show slower response decays when Na/Ca exchange was blocked. (*B*) The predicted effect of adding a surface pump equivalent to 0.001 cm/s to our model for simulating membrane currents in response to flash photolysis of nitr. The dashed line includes the pump; the solid line does not. This simulation is for the fifth 200-J flash at 1/2 min^{-1} in a 300-μm cell injected with 10 mM nitr-5, 75% Ca-loaded.

average reversal potential for $I_{NS(Ca)}$, so the recorded current should consist of nearly pure $I_{K(Ca)}$. When we replaced sodium either with TMA or lithium, flash-evoked $I_{K(Ca)}$ decays more slowly. Replacing Na with Li or TMA has no direct effect on $I_{K(Ca)}$ to voltage-clamp pulses. Replacing Na with Li also has no effect on the conductance or reversal potential of $I_{NS(Ca)}$ when $I_{K(Ca)}$ is blocked with TEA (unpublished observations). Replacing Na with TMA reduces the conductance underlying $I_{NS(Ca)}$, and shifts the reversal potential slightly (Kramer and Zucker, 1985*a*). Therefore, $I_{NS(Ca)}$ should remain a negligible component of the membrane current. The only expected effect of these ionic substitutions is to prevent calcium efflux via Na/Ca exchange (Requena and Mullins, 1979). Consequently the results illustrated in Fig. 13 *A* suggest that Na/Ca exchange contributes to the removal of calcium released near the membrane by flash photolysis.

We tried to estimate the magnitude of Na/Ca transport needed to achieve the effect observed. To do this, we modified Model 2 of the Appendix to include at front and rear surfaces a surface pump which removes total calcium at a rate proportional to free submembrane calcium. Measurements of calcium extrusion in the squid giant axon indicate a pump rate of about 1 pmol/cm^2·s per μM calcium, or 0.001 cm/s (Requena, 1983). Due to surface infoldings in *Aplysia* (Graubard, 1975), this figure needs to be increased severalfold. Moreover, our cubic cell model only has provision for extrusion at front and rear surfaces (one-third the total surface), so we must boost removal by another factor of 3 in our model. Fig. 13 *B* shows the effect of extruding calcium at the front and rear surfaces at a rate of 0.01 cm/s. Minor adjustments to the pump rate could be made to achieve a better fit to any particular data set, but the conclusion is clear: blocking a surface pump similar to that expected for neuronal membranes should have an effect on nitr responses similar to that actually observed by treatments that prevent Na/Ca exchange.

Relative stoichiometries of $I_{K(Ca)}$ and $I_{NS(Ca)}$. The above results indicate that the decay of membrane currents elicited by release of "caged calcium" are affected by calcium stoichiometry, nitr concentration, and surface pumps. The latter two effects can be controlled by separately recording $I_{K(Ca)}$ and $I_{NS(Ca)}$ in single cells filled with one nitr concentration, and under conditions that do not affect the operation of the Na/Ca exchanger. Fig. 14 illustrates two such experiments. In *A*, the trace marked "ASW" is a flash response in normal seawater which consists predominantly of $I_{K(Ca)}$, since $I_{NS(Ca)}$ is very small at -30 mV. The response marked "TEA" was obtained at the same potential in the presence of 50 mM TEA to block $I_{K(Ca)}$, and consists of the small amount of $I_{NS(Ca)}$ that was presumably present in the other trace. In *B*, $I_{K(Ca)}$ is recorded in isolation from another cell at -22 mV, the reversal potential for $I_{NS(Ca)}$, and $I_{NS(Ca)}$ is recorded at -70 mV, the reversal potential for $I_{K(Ca)}$. In both experiments, when the two currents are scaled to the same magnitude at 1 s, they are seen to decay at similar rates. Therefore, whatever the cooperativity of calcium action, it is similar for both currents. We obtained similar results in eight experiments.

Effect of voltage. The calcium-activated potassium channel has been shown to be strongly voltage-dependent in each system that has been studied. This voltage dependence may be due to voltage-dependent calcium binding (Gorman and Thomas, 1980; Barrett et al., 1982; Wong, et al., 1982; Moczydlowski and Latorre, 1983). One possibility is that more than one calcium ion may activate a channel by

binding at different sites, and that one or more of the sites might display voltage sensitivity. Then the apparent cooperativity of calcium action would be voltage dependent. This possibility confounds the interpretation of Fig. 14 *B*, where differences in decay rate of $I_{K(Ca)}$ and $I_{NS(Ca)}$ might be obscured by an effect of voltage.

Fig. 15 shows $I_{K(Ca)}$ and $I_{NS(Ca)}$ responses in a neuron recorded at potentials between −5 and −40 mV. The decay rates are unaffected by voltage. In 10 experiments on $I_{K(Ca)}$ and 6 experiments on $I_{NS(Ca)}$ we found no evidence of a voltage-dependent calcium cooperativity, and no indication of different voltage-sensitive calcium binding at multiple binding sites.

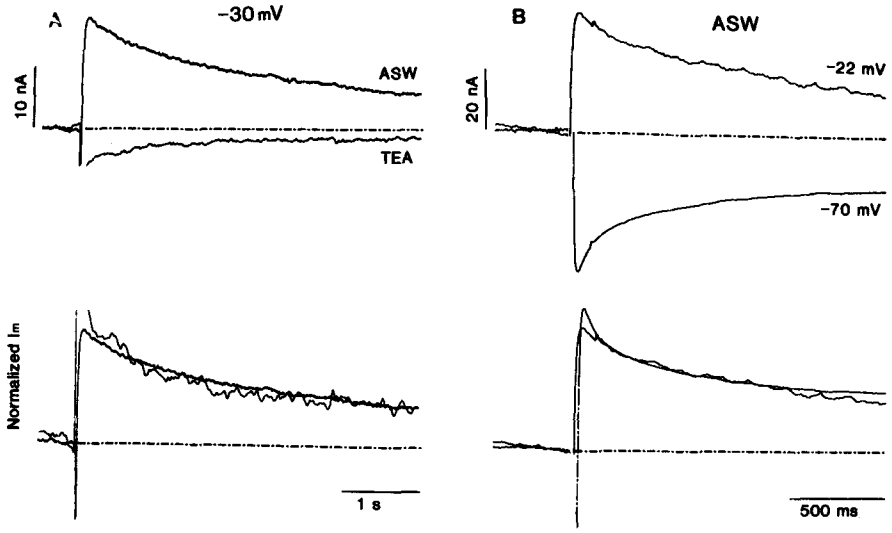

FIGURE 14. $I_{K(Ca)}$ and $I_{NS(Ca)}$ evoked by 200-J flashes in neurons filled with 10 mM nitr-5, 80% loaded with calcium. The cell in *A* was clamped to −30 mV. The trace marked "ASW" was obtained in normal artificial seawater. Since −30 mV is near the reversal potential for $I_{NS(Ca)}$, this current is predominantly carried by $I_{K(Ca)}$. The trace marked "TEA" was obtained in normal medium with 50 mM TEA added to block $I_{K(Ca)}$. The remaining current is the $I_{NS(Ca)}$ evoked by a flash at −30 mV. (*B*) $I_{K(Ca)}$ was isolated by clamping a different cell at −22 mV, the reversal potential for $I_{NS(Ca)}$; $I_{NS(Ca)}$ was isolated by clamping the cell at −70 mV, the reversal potential for $I_{K(Ca)}$. In both cells, the currents were normalized to the same peak and superimposed to show that $I_{K(Ca)}$ and $I_{NS(Ca)}$ responses decay at the same rate, suggesting similar calcium activation stoichiometries.

Determinants of Tail Current Duration after a Burst

The results so far indicate that both $I_{K(Ca)}$ and $I_{NS(Ca)}$ depend linearly upon submembrane calcium activity. During a burst of action potentials (Gorman and Thomas, 1978) or a depolarizing pulse (Ahmed and Connor, 1979; Gorman and Thomas, 1980; Smith and Zucker, 1980), calcium accumulates beneath the membrane. This submembrane calcium dissipates after the burst or pulse. The decay of this surface calcium ought to govern the decay of both $I_{K(Ca)}$ and $I_{NS(Ca)}$. Why, then, do these currents decay at different rates?

One difference between $I_{K(Ca)}$ and $I_{NS(Ca)}$ is that the conductance underlying the former has a marked voltage-dependence in *Aplysia* (Gorman and Thomas, 1980), while the conductance of the latter is voltage-independent (Kramer and Zucker, 1985*a*; Swandulla and Lux, 1985). Thus voltage-dependent relaxation of $I_{K(Ca)}$ should contribute to the time course of $I_{K(Ca)}$, but not to that of $I_{NS(Ca)}$.

Molecular model of $I_{K(Ca)}$. To formulate the interaction of calcium and voltage in governing $I_{K(Ca)}$, we used the simplest possible reaction scheme for the activation of $I_{K(Ca)}$.

$$X + Ca \underset{\alpha}{\overset{\beta}{\rightleftharpoons}} CaX, \tag{1}$$

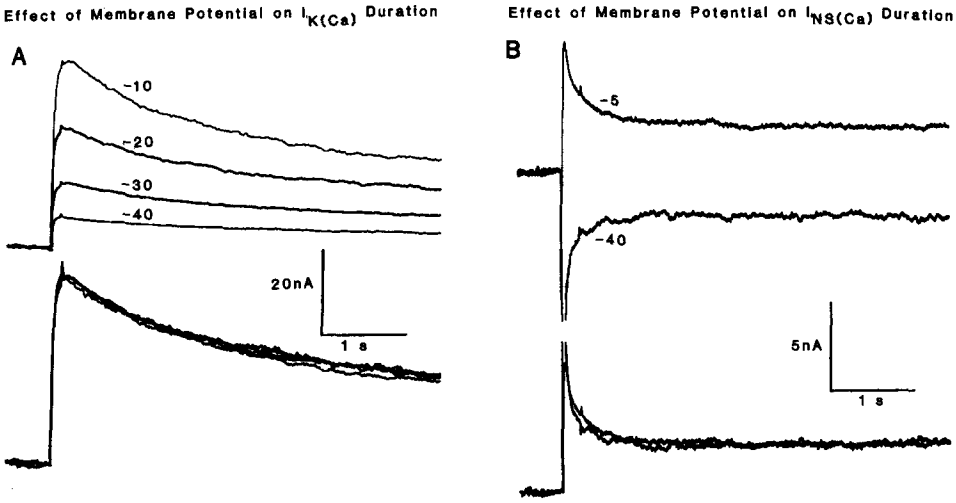

FIGURE 15. (*A*) $I_{K(Ca)}$ responses at different membrane potentials (indicated by the numbers next to the traces) to 100-J flashes in a neuron filled with 10 mM nitr-5 75% Ca-loaded. $I_{NS(Ca)}$ was minimized by using a Co-substituted Ca-free, TMA-substituted Na-free medium. (*B*) $I_{NS(Ca)}$ at different membrane potentials to 200-J flashes in a different neuron injected with the same nitr mixture as in *A*. $I_{K(Ca)}$ was blocked with 50 mM TEA. In both experiments, the responses obtained at different voltages are shown separately at the top, and superimposed after normalization below. Current calibrations apply to the unnormalized responses.

where X is the receptor for calcium, $Ca(t)$ is the submembrane calcium concentration as a function of time, α is the closing rate of the channel, β is the opening rate of the channel, and α and β are assumed to be functions of voltage. Let a neuron contain N channels that can contribute to generating $I_{K(Ca)}$, and y be the number of these channels that are open. The y is governed by the equation:

$$dy/dt = \beta Ca(t)(N - y) - \alpha y = \beta NCa(t) - [\alpha + \beta Ca(t)]y. \tag{2}$$

Consider first the situation where the voltage is suddenly changed from one level to another. If α and β are relatively fast, and $Ca(t)$ is changing slowly with time, we may

consider that $Ca(t)$ remains constant. Then Eq. 2 becomes

$$dy/dt = \beta NCa - (\alpha + \beta Ca)y. \tag{3}$$

After a voltage step that changes α and β, y relaxes with rate constant $\alpha + \beta Ca$ to a new steady-state level,

$$y(t = \infty) = \frac{\beta Ca}{\alpha} \frac{N}{(1 + \beta Ca)/\alpha} \tag{4}$$

This steady-state level of the number of open channels is a saturating function of Ca. However, we observed no saturation of the calcium dependence of $I_{K(Ca)}$ in concentration jump experiments (Fig. 8). Therefore, in our experiments, βCa must remain less than α, in which case y relaxes with rate constant α, and Eq. 3 reduces to

$$dy/dt = \beta NCa - \alpha y. \tag{5}$$

If the open channels have uniform conductance γ, the membrane potential is V, and the equilibrium potential for potassium is E, the macroscopic $I_{K(Ca)}$ current through the channel when Ca is constant will be given by

$$dI/dt = \beta NCa\gamma(V - E) - \alpha I. \tag{6}$$

The current will relax exponentially with rate constant α to the steady-state level $\beta NCa\gamma(V - E)/\alpha$.

α may be estimated directly from the relaxation of $I_{K(Ca)}$ after a voltage step. βN may be estimated from the steady-state currents before and after a voltage step. Consider a change in membrane potential from V_1 to V_2. The steady-state change in $I_{K(Ca)}$, ΔI, is given by

$$\Delta I = \beta_2 NCa\gamma(V_2 - E)/\alpha_2 - \beta_1 NCa\gamma(V_1 - E)/\alpha_1, \tag{7}$$

where the subscripts refer to the voltages to which the rate constants pertain. To this current must be added currents through other conductances present in the membrane. The currents through calcium-independent conductances can be eliminated by repeating the voltage step at two different intracellular calcium concentrations (e.g., before and after release of "caged calcium" by flash photolysis). Then the difference in current is given by

$$\Delta I = \Delta Ca[\beta_2 N\gamma(V_2 - E)/\alpha_2 - \beta_1 N\gamma(V_1 - E)/\alpha_1], \tag{8}$$

where ΔCa refers to the change in calcium concentration caused by the flash.

The only unknowns in Eq. 8 are $\beta_1 N$, $\beta_2 N$, γ. By keeping track of the flash exposure history, the calcium concentration change caused at the front surface by a flash can be estimated using Model 1. Suppose a voltage step occurs 0.5 s after a flash. From 16 *A*, we estimate that at 0.5 s the calcium increment at the front of the cell drops ~25% of the way from its peak at the flash to its steady-state level after diffusional equilibration. Therefore, we corrected the predicted change in front surface calcium to account for this decline at the time of a voltage step in applying Eq. 8. The single channel conductance of the calcium-activated potassium channel sensitive to TEA in *Aplysia* has been measured as about 20 pS in normal potassium con-

centrations (Levitan, I. R., and A. Hermann, personal communications; see also Lux et al., 1981; Hermann and Hartung, 1982; and Ewald et al., 1985).

Another estimate of βN can be obtained from the peak level of the flash response at a particular voltage. This incremental current is given by

$$\Delta I = \beta N \Delta Ca \gamma (V - E)/\alpha. \tag{9}$$

Rate constants for $I_{K(Ca)}$ reaction scheme. Fig. 16 illustrates an experiment in which the flash response and incremental calcium-dependent current was used to estimate

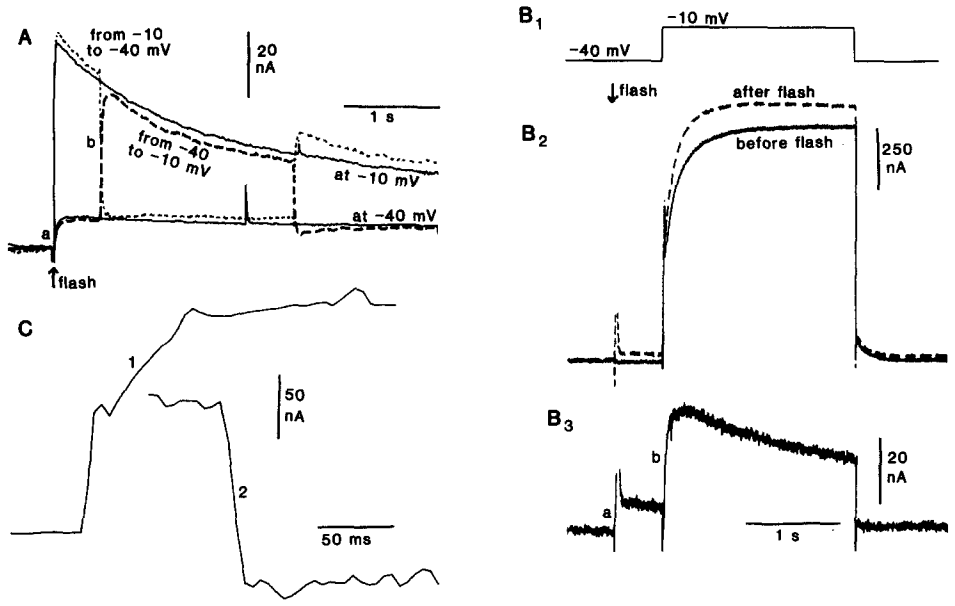

FIGURE 16. Data used to estimate rate constants in the reaction scheme for $I_{K(Ca)}$, in a neuron filled with 10 mM nitr-5 and 8.5 mM calcium. (*A*) Flash responses at −10 and −40 mV (*solid lines*), and effect of pulses from −40 to −10 mV (*dashed line*) and from −10 to −40 mV (*dotted line*). Current filtered with 10-ms time constant. (*B*) Extraction of unfiltered calcium-dependent membrane current (B_3) from total current records (B_2) before (*solid line*) and after a flash (*dashed line*). The voltage pulse is shown in B_1. Filtering the record of B_3 provided the dashed trace in *A*. *a* and *b* mark the current increments used to estimate the forward rate constant, as described in the text. (*C*) $I_{K(Ca)}$, extracted as in *B*, to steps to −10 mV (*1*) and to −40 mV (2). Note the faster time scale. Records digitally smoothed with 2.5-ms time constant.

βN at two different voltages. An upper left quadrant burster from an *Aplysia* abdominal ganglion was injected with 10 mM nitr-5, 85% loaded with calcium. $I_{NS(Ca)}$ was minimized by using a zero-calcium, zero-sodium medium. The upper solid line in *A* shows the response to a 150-J flash when the membrane potential was clamped at −10 mV. The lower solid line shows the flash response at −40 mV. The dashed line shows the change in calcium-dependent current in stepping from −40 to −10 mV for 2 s. The dotted line shows the change in $I_{K(Ca)}$ in stepping from −10 to −40 mV for 2 s.

Fig. 16 *B* illustrates how we obtained the voltage-dependent changes in $I_{K(Ca)}$ shown as dotted and dashed lines in *A*. The total current on stepping from −40 to −10 mV and back before a flash was subtracted from the total current accompanying an identical pulse after a flash. $I_{K(Ca)}$ is only 15% of the total current, so it seemed possible that extracting this current accurately from the net current might be subject to large error. That this was not the case is evident from Fig. 16 *A*, which shows that the extracted change in $I_{K(Ca)}$ caused by a voltage step superimposes nicely on the flash responses obtained separately at the two voltages. Our analysis was based only on those experiments in which this control confirmed the accuracy of our extraction procedure.

The incremental current marked *a* in Fig. 16, *A* and *B*, corresponds to the current of Eq. 9. From this we can calculate a value for βN at −40 mV. This plus the current step marked *b* in Fig. 8 can be used with Eq. 8 to calculate a value for βN at −10 mV. This agrees with the estimate using the flash response at −10 mV and Eq. 9.

The above procedures assume that $I_{NS(Ca)}$ has been entirely eliminated in the medium lacking sodium and calcium. However, even TMA appears to permeate the nonspecific cation channel slightly (Kramer and Zucker, 1985*a*; Swandulla and Lux, 1985). In TMA medium, $I_{NS(Ca)}$ has a reversal potential of about −40 mV, so it should not contribute to the flash response at this potential (*a* in Fig. 8), but might form a part of the calcium-dependent current on stepping from −40 to −10 mV. To check for the presence of $I_{NS(Ca)}$, we looked for a flash response at −80 mV in each experiment. This is near the potassium reversal potential, and at a level at which the calcium-dependent potassium conductance is not activated (Gorman and Thomas, 1980), and so should provide a direct indication of $I_{NS(Ca)}$. In some experiments, a small response was detected. The $I_{NS(Ca)}$ expected for a step from −40 to −10 mV was calculated and subtracted from *b* before applying Eq. 8. In most cells, this amounted to about a 10% correction.

The rate constant α was determined from the relaxation rate of $I_{K(Ca)}$ after voltage steps to −10 mV and to −40 mV. For this purpose, we used unfiltered current records (Fig. 8 *B*), and usually replotted the records at a faster sweep speed (Fig. 8 *C*).

Our results from five experiments are that α was 92 ± 11 s^{-1} (±SD) at −40 mV and 49 ± 10 s^{-1} at −10 mV. βN was 1.3 ± 0.6 × 10^{11} M^{-1} s^{-1} at −40 mV and 2.2 ± 0.8 × 10^{11} M^{-1} s^{-1} at −10 mV. Since these currents originated from only the front surface of a cell, we expect that only half the somatic $I_{K(Ca)}$ channels were activated. For the whole cell, βN should be doubled.

Another measure of the rate constant might be provided by the rising phase of the flash response at different voltages, if a flash changes the surface calcium concentration rapidly compared with α. We found that the $I_{K(Ca)}$ evoked by a flash rose to a peak with a time constant of ~30 ms at all voltages. This was generally slower than the relaxation of responses to voltage steps, suggesting that the calcium concentration did not change as fast as expected from the photolysis rate for nitr-5 (0.3 ms, Adams et al., 1988). Perhaps the extensive surface infolding of *Aplysia* neural membrane (Graubard, 1975) produces tortuous diffusion pathways between surface fingers of cytoplasm where nitr is photolyzed and deeper membrane folds where

calcium-dependent channels are located. Rising phases of flash responses were also distorted by electromagnetic, mechanical, and photolytic artefacts generated by the intense flashlamp discharge (Tsien and Zucker, 1986). We therefore felt that flash responses provided a poorer estimate of α than the responses to a voltage step.

Rate constants for the $I_{NS(Ca)}$ reaction scheme. Eq. 1 should apply equally well to the activation of $I_{NS(Ca)}$. The same procedures should allow estimation of rate constants for this current. We therefore repeated the experiment of Fig. 16 on $I_{NS(Ca)}$, after blocking $I_{K(Ca)}$ with 50 mM TEA. The nonspecific cation current, extracted by the same procedure as in Fig. 16 *B*, was found to relax with time constants of less than 10 ms at all voltages. Since our cells were not axotomized, this is close to the relaxation of the capacitance current. We were therefore unable to extract estimates of $I_{NS(Ca)}$ channel lifetime from our relaxation measurements, and can only conclude that current through these channels reaches equilibrium much more rapidly than is the case for the $I_{K(Ca)}$ channels. It has also been shown that the conductance underlying $I_{NS(Ca)}$ is not voltage dependent (Kramer and Zucker, 1985*a*; Swandulla and Lux, 1985), so that voltage-dependent relaxations should not occur at all for this current. Taken together, these results imply that the $I_{NS(Ca)}$ tail current after a voltage pulse should accurately follow the time course of the change in submembrane calcium. Postpulse tail currents of $I_{K(Ca)}$, however, should contain both voltage-dependent and calcium-dependent relaxations.

Prediction of calcium-dependent tail currents. The calcium-activated potassium tail current after a voltage pulse should be given by the solution to Eq. 6, only now *Ca* is a function of time. Smith and Zucker (1980) and Barish and Thompson (1983) have described a procedure for estimating the time course of submembrane calcium concentration during and after a depolarizing pulse. In this procedure, the diffusion equation is solved in spherical coordinates with a number of boundary conditions. Diffusion is assumed to occur with binding to saturable but immobile buffer sites throughout cytoplasm. We used 1.5 mM of a buffer with 25 μM dissociation constant, consistent with measurements of the ratio of free to total calcium in these neurons (Smith and Zucker, 1980). Calcium was extruded by a combination of surface membrane pump and organelle uptake systems. The surface pump had a maximum rate of 3.5 pM/cm^2·s, or 25 pM/cm^2·s after accounting for surface infolding, and saturation constant 2 μM. The uptake pump had a forward rate constant of 20 μM^{-1} s^{-1}, a backward rate of 0.08 s^{-1}, and a capacity of 0.5 mM. These values are consistent with measurements of these pumps in neurons (Blaustein et al., 1978*a*, *b*; Requena, 1983), and together they can remove calcium from cytoplasm at the rate measured after a depolarizing pulse (Smith and Zucker, 1980). Organelles are preloaded, and a membrane leak is provided, so that the steady-state free calcium concentration is 200 nM (Gorman et al., 1984). Calcium influx is described by a Hodgkin-Huxley (1952) system of equations. Activation is second order with a 7-ms time constant approaching a peak current of 975 nA. Inactivation is first order with a 200-ms time constant approaching 22% the peak current. We chose these values to provide a good fit to our (unpublished) records of calcium current in these neurons during a pulse to −10 mV. The values are very similar to those described previously for the calcium current in *Aplysia* (Chad et al., 1984).

Using finite difference methods, the diffusion equation with these boundary con-

ditions was solved for a 100-ms pulse. Fig. 17 *A* shows the predicted calcium concentration as a function of time after this pulse, at a distance of one micron beneath the cell membrane. We chose a 1-μm distance to represent the situation that calcium must diffuse some distance from calcium channel mouths before acting on calcium-dependent channels. It can be seen from the figure that the predicted decay of submembrane calcium concentration is very close to the observed time course of $I_{NS(Ca)}$ tail current following a pulse. Starting with the tail current amplitude 100 ms

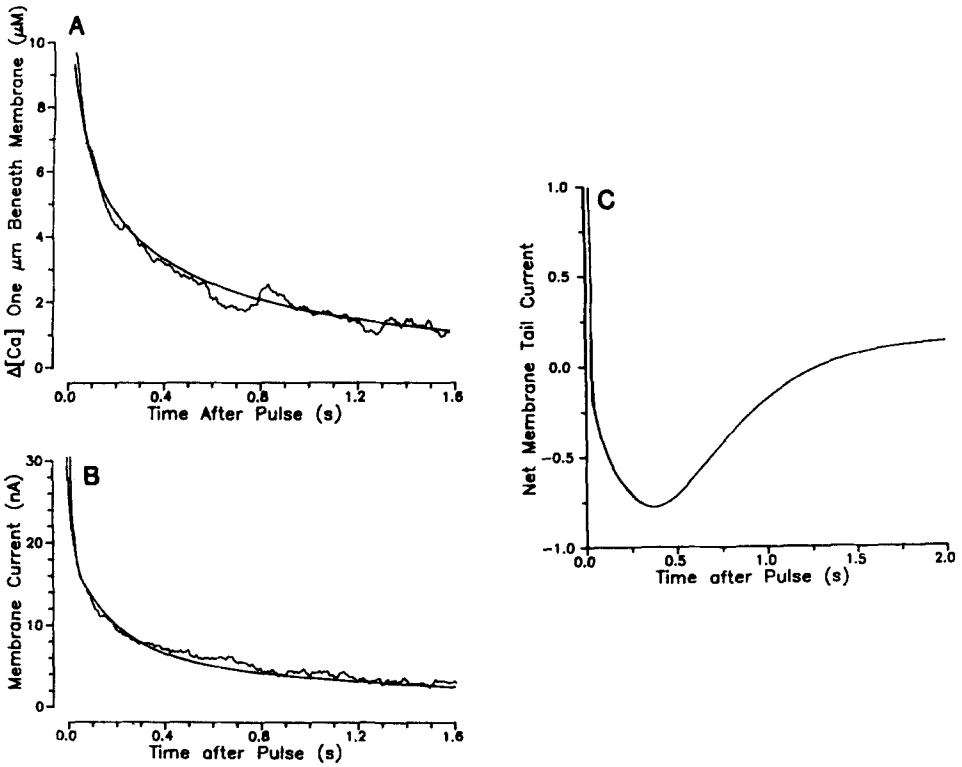

FIGURE 17. (*A*) Predicted decay of free calcium concentration in a spherical shell 1 μm below the surface, after a 100-ms pulse to −10 mV (*smooth curve*), using the model for calcium diffusion in spherical coordinates with binding, extrusion, uptake, and influx described in the text. This is compared to an example of $I_{NS(Ca)}$ following a 100-ms pulse to −10 mV (*noisy curve*). Potassium currents were eliminated with 50 mM TEA and by clamping to the potassium equilibrium potential (−77 mV). Inward current plotted upward, and smoothed with 15-ms time constant. (*B*) Predicted decay of $I_{K(Ca)}$ after a 100-ms pulse to −10 mV (*smooth curve*), based on the change in submembrane calcium concentration calculated in *A* and the voltage-dependent relaxations illustrated in Fig. 8. An example of $I_{K(Ca)}$ after such a depolarization, smoothed with 15-ms time constant (*noisy curve*) is also shown. The experimental curve is the difference between tail currents before and after exposure to 3 mM TEA, recorded at −40 mV. In both *A* and *B*, the experimental curves were scaled to the same magnitude as the predictions. Outward current plotted upward. (*C*) Net postdepolarization tail current obtained by scaling and mixing the predicted currents from *A* and *B*.

after the end of the pulse, both observed and predicted current drop to half this level 360 ms later.

A prediction of $I_{K(Ca)}$ tail current was obtained by solving Eq. 6 for the calcium time course of Fig. 17 *A*. To do this analytically, we fitted the submembrane calcium time course after a pulse with a sum of three exponentials:

$$Ca(t) = c_o + \sum_{i=1}^{3} c_i e^{-\delta_i t}. \tag{10}$$

Then the solution to Eq. 6 is given by

$$I = \beta_{40} N\gamma (V - E)\cdot\left[\frac{c_o}{\alpha_{40}} - \left(\frac{c_o}{\alpha_{40}} + \sum_{i=1}^{3} \frac{c_i}{\alpha_{40} - \delta_i} e^{-\alpha_{40} t} + \sum_{i=1}^{3} \frac{c_i e^{-\delta_i t}}{\alpha_{40} - \delta_i}\right)\right] + G_o (V - E) e^{-\alpha_{40} t}, \tag{11}$$

where G_o is the macroscopic conductance of the calcium-activated potassium channels immediately following the pulse. This is not a steady-state value of conductance of underlying $I_{K(Ca)}$, because the calcium concentration has been rising throughout the pulse. To estimate G_o we plotted the predicted time course of free calcium 1 μm from the surface during the pulse and fitted it to the approximate equation $Ca = Ca_o + At$, rising (after an early sigmoidal rise which we represent as a 22-ms delay) to 9.5 μM in 78 ms from a resting level (Ca_0) of 200 nM. For such a calcium concentration as a function of time, the conductance during the pulse will rise according to

$$G(t) = \beta_{10} N\gamma \cdot \left\{\frac{c_o}{\alpha_{10}} (1 - e^{-\alpha_{10} t}) + \frac{A}{\alpha_{10}^2} [\alpha_{10} t - (1 - e^{-\alpha_{10} t})]\right\} + \frac{\beta_{40} N\gamma c_o e^{-\alpha_{10} t}}{\alpha_{40}}. \tag{12}$$

This equation was solved for $t = 78$ ms to obtain an estimate of G_o at the end of the pulse. Then Eq. 11 was used to generate a prediction of the $I_{K(Ca)}$ tail current.

The result of this simulation is presented in Fig. 17 *B*. We also show an example of $I_{K(Ca)}$ after a 100-ms pulse to ~ -10 mV. The recorded tail current was confined to $I_{K(Ca)}$ by recording the difference between currents before and after perfusing with 3 mM TEA. $I_{NS(Ca)}$ was minimized by using zero-sodium seawater. We confirmed that the tail current was really $I_{K(Ca)}$ by showing that it reversed at the potassium equilibrium potential, and that it was absent in zero-calcium solution (data not shown). The predicted time course is similar to that of the observed current. The curves drop to half the 100-ms level after an additional 250 ms. This is somewhat faster than the decay of $I_{NS(Ca)}$.

Our prediction also provides an absolute magnitude of the expected tail current in a "typical" cell. We expect to see 14 nA of $I_{K(Ca)}$ 100 ms after the pulse. Our currents are smaller than this (range 4–7.5 nA), but this is because we isolated $I_{K(Ca)}$ as the current blocked by 3 mM TEA. This weak dose of TEA does not remove $I_{K(Ca)}$ completely (Hermann and Gorman, 1981); in our hands, a 5-min perfusion blocks only 50% of $I_{K(Ca)}$. However, higher doses block substantial amounts of the delayed rectifier current (Hermann and Gorman, 1981), which would distort the time course of $I_{K(Ca)}$. Thus, we must expect our procedure to report only a fraction of the total level of $I_{K(Ca)}$ in the cell.

Reconstruction of net tail current after a pulse. The current after a depolarization normally consists of a mixture of $I_{K(Ca)}$ and $I_{NS(Ca)}$, as well as a late outward current due to inactivation of calcium channels (Adams, 1985; Adams and Levitan, 1985; Kramer and Zucker, 1985*a*, *b*). By scaling and mixing the predicted time courses of $I_{K(Ca)}$ and $I_{NS(Ca)}$, we should be able to reconstruct a waveform that resembles the first two phases of tail current in the normal sequence. Fig. 17 *C* shows such a reconstruction. The initial outward tail quickly turns into an inward tail that persists for 1 s or longer, much like the first two phases of tail current after a burst of action potentials or a depolarizing pulse (for numerous examples, see Kramer and Zucker, 1985*a*).

DISCUSSION

Complexity of Nitr Chemistry

The first part of our study outlines the behavior of mixtures of calcium buffers to repeated photolytic conversions of a high-affinity buffer to a low-affinity form. Measurements of calcium concentration changes in vitro using arsenazo III spectrophotometry revealed numerous complications. Successive flashes convert diminishing amounts of nitrobenzhydrol to nitrosobenzophenone. The amount converted by each flash declines as the nitrobenzhydrol available for conversion is exhausted. Even the average percentage of nitrobenzyhydrol converted declines, because the low-affinity and photolytically inert nitrosobenzophenone is much darker than the nitrobenzhydrol, so that the average light intensity in a cuvette (or cell) drops with successive flashes. Only at the front surface of the cuvette (or cell) is the percentage of nitr photolysis constant for a given flash intensity.

Despite these reductions in nitr photolysis with successive flashes, the increments in both volume-average and front-surface free calcium concentration grow for the first few flashes. Successive flashes bring the high-affinity nitrobenzyhydrol closer to saturation, as the total calcium remains constant while the amount of this buffer drops. A saturated buffer releases more calcium than a nonsaturated buffer, for a given reduction in amount of buffer. This accounts for the rise in calcium concentration increments, until the nitrobenzhydrol becomes almost fully saturated. Subsequent calcium increments decline as the nitrobenzhydrol is exhausted.

A quantitative description of these processes requires computer simulations which take account of the effects of calcium equilibration among multiple buffers of changing composition, the effects of changing absorbance of the mixture of buffers on average light intensity, and the differential quantum efficiencies of free and calcium-bond nitrobenzhydrol. This model is validated by measurements of calcium concentration change in vitro and in vivo. It shows that more highly loaded nitr mixtures initially cause larger calcium concentration jumps, more rapid approach to peak calcium releases, and faster subsequent drops in response to flashes. Increased buffer concentration reduces the average light intensity, slowing the exhaustion of nitr and reducing the average calcium increments, while the surface effects of light flashes are little affected. Naturally, brighter flashes release more calcium, and the peak change in incremental calcium occurs sooner.

Consideration of Calcium Extrusion

Cells are equipped with calcium extrusion mechanisms that ought to function in cells injected with nitr. As long as the free calcium concentration is elevated over its normal level, these pumps will act to remove the calcium that was injected with the nitr. Since the pump must operate against a large quantity of an unusually powerful buffer, injected calcium will be reduced very slowly, compared to the rate of removal of injected unbuffered calcium, or the rate of removal of calcium that enters normal cells through voltage-dependent channels. In cells filled with 10 mM nitr, half the 7.5 mM calcium that we inject is pumped out of cytoplasm in ~90 min; at least, this is how we account for the drop in membrane current responses in cells during such a pause in flash photolysis.

This pump rate may be compared to calcium extrusion systems that have been described in neurons. Blaustein et al. (1976*a*, *b*) describe a nonmitochondrial uptake system that would remove calcium at near its maximal rate of 2 μM/s in cells filled with nitr and having free calcium levels above 1 μM. After 10 200-J flashes, a cell injected with 10 mM nitr 75%-loaded with calcium has an effective buffer ratio of total to free calcium of ~1,500. The nonmitochondrial sequestration system will extrude 4.5 mM calcium in 90 min, close to what we observe. Alternatively, Requena (1983) reviews the properties of surface pumps which remove calcium at a rate of 1 pM/cm^2·s per μM free calcium, or 0.001 cm/s. Considering the size of our cells, and the buffer ratio of 1,500, this corresponds to a time constant of 110 min, which again is similar to what we observe. Either system would remove calcium at a rate consistent with the rate at which resting cells lose their ability to generate calcium-dependent responses to nitr photolysis. Blocking Na/Ca surface exchange slows the decay of membrane currents by an amount similar to that expected for an extrusion rate of 0.001 cm/s, suggesting that this may be the main mechanism used to restore calcium levels to normal when these neurons are filled with "caged calcium."

Measurements of Calcium Stoichiometry

One limitation of the use of nitr compounds to study calcium dependence of physiological responses is the high resting level of free calcium in nitr mixtures. The free calcium concentration can be reduced by loading nitr with less calcium, but then the increments in calcium caused by flash photolysis are also smaller. Increased loading of nitr with calcium increases the photolytic calcium increments faster than it increases the initial resting level of calcium, but too high a loading tends to put the calcium out of effective control by the nitr buffer. The optimum loading is ~75–85%.

The initial calcium level can be reduced by using the higher affinity form of nitr, nitr-7. However, the calcium increments on flash photolysis are proportionately reduced in nitr-7, with the same achievable percentage increase in calcium concentration as nitr-5.

Measurements of calcium stoichiometry require changes in calcium concentration that are greater than the initial level. Because calcium accumulates with repeated nitr photolysis, this situation can only be achieved by using a few flashes of widely different intensity, beginning with the dimmest flash. Any other procedure is likely

to erroneously indicate a linear relation between response and flash intensity for any stoichiometry.

Calcium Stoichiometry of $I_{K(Ca)}$

Calcium-activated potassium currents have been observed in a wide variety of cells (Thompson and Aldrich, 1980). The stoichiometry of calcium action has been studied using single channel recordings of this current in membrane patches from rat muscle and clonal pituitary cells (Barrett et al., 1982; Methfessel and Boheim, 1982; Wong et al., 1982; Moczydlowski and Latorre, 1983). These studies indicate that at least two and probably three calcium ions are involved in activation of this current in these muscle and tissue culture cells. It should be noted that the $I_{K(Ca)}$ channel that we have studied in molluscan neurons is quite different from that found in mammalian muscle and clonal pituitary cells. The latter has a single-channel conductance of >100 pS, while the former has a single-channel conductance of about 20 pS in normal potassium concentrations (Lux et al., 1981).

In contrast, experiments on whole cell recording of $I_{K(Ca)}$ in molluscan neurons usually show a linear relationship between the membrane current and magnitude of calcium injection (Gorman and Thomas, 1980; Hermann and Hartung, 1982). Using nitr to raise calcium, Gurney et al. (1987) have recently described a $I_{K(Ca)}$ in sympathetic neurons that is activated linearly by calcium jumps. Meech and Thomas (1980), however, found a third-power dependence of $I_{K(Ca)}$ upon quantity of calcium injected in snail neurons. This nonlinearity was only evident for massive calcium injections (greater than 3 mM final concentration of calcium injected), which would probably saturate buffers and raise the free calcium concentration to >100 μM. Weaker injections, similar to those used in the other studies, elicited currents that appeared to depend linearly upon calcium injected.

Our results using "caged calcium" indicate a linear, nonsaturating relationship between $I_{K(Ca)}$ and calcium concentration jump in the range 0.1–20 μM. It is possible that a nonlinearity, reflecting the binding of additional calcium ions with low affinity, would show up at higher calcium concentrations than are achievable using nitr buffers.

For a train of repeated flashes, the rise and subsequent fall in calcium increments measured in vitro with arsenazo III is mirrored by a similar pattern of increments in $I_{K(Ca)}$ in neurons. These data are also consistent only with a first-order calcium cooperativity. The drop in response amplitudes could reflect a block of $I_{K(Ca)}$ by high calcium levels, as reported for transverse tubule channels (Vergara and Latorre, 1984). In muscle, calcium block occurred only for [Ca] > 100 μM, and the binding site had very low affinity (K_D = 0.29 M). Such a low affinity and our ability to account for the decline in $I_{K(Ca)}$ increments from exhaustion of nitr argue against this explanation.

The conductance underlying $I_{K(Ca)}$ is highly voltage-sensitive (Gorman and Thomas, 1980; Kostyuk et al., 1980; Hermann and Hartung, 1982; Lux and Hofmeier, 1982*a*, *b*), and this voltage dependence may arise from voltage-dependent binding of calcium to its receptor. We therefore looked for a voltage dependence of calcium stoichiometry in activating $I_{K(Ca)}$. We found none in the range −30 to −10 mV.

Our most robust responses are in the range expected for normal physiological activation of $I_{K(Ca)}$. For example, consider the results from two cells included in Fig. 8. In one filled with 20 mM nitr-5, 75%-calcium loaded, a 6 μM calcium jump at the front surface activated 115 nA of $I_{K(Ca)}$ at −22 mV. If the back surface had been activated too, we should have observed 230 nA. Considering the voltage dependence of $I_{K(Ca)}$ (Gorman and Thomas, 1980), this would correspond to ~0.6 μA at 0 mV. In another cell filled with 20 mM nitr-5, 90%-calcium loaded, a 20 μM calcium jump at the front surface activated 125 nA at −30 mV. After doubling for the whole cell surface and correcting for voltage dependence, this corresponds to 1.5 μA at 0 mV. Thus we evoke ~100 nA $I_{K(Ca)}$ per μM calcium jump (at 0 mV). The 1.5 μA caused by the 20 μM jump is similar to the level of $I_{K(Ca)}$, which we observe in left upper quadrant bursters during brief voltage clamp steps. This is intermediate between reported levels of this current in cells R15 and L11 (Gorman and Hermann, 1982). The calculated calcium jump of 20 μM is also similar to the 10 μM rise in free calcium that we estimate occurs within 1 μM of the surface after a 100-ms depolarization to 0 mV. Thus we feel that the calcium released by light flashes in cells filled with nitr is in the normal physiological range occurring during nervous activity, and the evoked $I_{K(Ca)}$ responses are also similar to those normally occurring in these neurons.

We conclude, therefore, that in this normal physiological range, only one calcium ion is required to activate $I_{K(Ca)}$.

Calcium Stoichiometry of $I_{NS(Ca)}$

This current was only recently discovered in a few tissues (Hofmeier and Lux, 1981; Petersen and Maruyama, 1984). Its calcium dependence has not yet been described. Our results indicate that $I_{NS(Ca)}$, too, is activated by a single calcium ion. This current is not voltage-activated (Kramer and Zucker, 1985*a*; Swandulla and Lux, 1985), and we found no voltage sensitivity to its calcium dependence.

The magnitude of the conductance (G) underlying this current is much smaller than that underlying $I_{K(Ca)}$. For example, in the best cells in Fig. 9, a 6 μM calcium jump evoked 0.15 μS of $G_{NS(Ca)}$. This contrasts to 2.3 μS of $G_{K(Ca)}$ at −22 mV in the best cells of Fig. 8. Since molluscan $I_{K(Ca)}$ channels and $I_{NS(Ca)}$ from other tissues have similar single channel conductances (Petersen and Maruyama, 1984), the difference in magnitude of whole-cell current could be due to differences in channel number, activation probability, open time, or calcium affinity.

Kinetics of Flash Responses

Our interest in the kinetics of the flash response arose from the hope that it could provide another indication of the stoichiometries of calcium activation of $I_{K(Ca)}$ and $I_{NS(Ca)}$ from the form of their decay after a flash photolysis release of "caged calcium." We believed that this decay was a stoichiometric measure of the removal of calcium from the submembrane space, caused primarily by diffusion of calcium formed near the surface facing the light into the darker interior where less photolytic calcium release occurred.

A slowly developing block of membrane current elicited by calcium increments was another possible cause for response decay. Calcium block has been reported in

$I_{K(Ca)}$ in muscle and pancreas (Vergara and Latorre, 1984; Findlay, et al., 1985), but only at very high calcium concentrations (>100 μM) or very positive membrane potentials (>+20 mV). Eckert and Ewald (1982) looked specifically for calcium-dependent inactivation of $I_{K(Ca)}$ in *Aplysia* neurons, and found none.

To treat diffusion as a determinant of response kinetics, we constructed a second model that encompassed the spatially dependent photolysis of nitr and the subsequent equilibration and diffusion of calcium and the various free and calcium-bound buffer constituents. Model 2 was only a rough approximation to reality, because we treated the cell as a cube with light impinging on one surface. Calcium actually diffuses from the front surface of a sphere toward the interior and the rear, and the vectorial direction of diffusion depends on the angular distance from the center of the front surface, the depth, and time after the flash. Diffusion is not unidimensional, and the accurate solution of this problem is much more complex than our approximation. Nevertheless, our approximation provided a good prediction of the time course of membrane currents assumed to be proportional to the submembrane calcium concentration. Since all parameters were estimated in advance, based on independent measurements, we feel this provides strong evidence for our contention that diffusion is the predominant process governing the decay of flash-evoked responses in these cells.

Our simulations showed that the decay rate was affected not only by the stoichiometry of calcium action, but also by nitr concentration and calcium extrusion. The variability of these factors in different cells prevents us from deducing stoichiometry from the decay rate of membrane currents elicited by release of caged calcium. Nevertheless, the fact that both $I_{K(Ca)}$ and $I_{NS(Ca)}$ decay at the same rate in a given cell indicate that these currents are activated by calcium with similar degrees of cooperativity. Preliminary results (Tsien and Zucker, 1986) suggesting different decay rates for $I_{K(Ca)}$ and $I_{NS(Ca)}$ responses were probably due to inadequate control of the many factors affecting response decay. Our present results further indicate that this stoichiometry is independent of voltage, since the decay rate of flash-evoked responses is unaffected by voltage. It is therefore unlikely that additional calcium ions bind to the receptors for these channels, at least in the range of voltages tested for each current.

Kinetics of Tail Currents after Bursts or Depolarizing Pulses

When the voltage across the cell membrane is changed, the binding of a single calcium ion to its receptor, as well as channel opening and closing rates, might be altered. This would result in a voltage-dependent relaxation of the channels to a new steady-state probability of being open, and to a new steady-state level of current, independent of any change in the calcium concentration. Channels subject to this influence would be governed by the kinetics of the voltage-dependent rate constants, as well as by the kinetics of calcium concentration change.

Such a situation would be manifest as a relaxation of conductance to a new steady-state level when the voltage is stepped to a new level. We detected no such relaxations in $I_{NS(Ca)}$, and its conductance appears to be independent of voltage (Kramer and Zucker, 1985*a*; Swandulla and Lux, 1985). However, $I_{K(Ca)}$ is well known to be voltage dependent as well as calcium dependent in *Aplysia* neurons

(Gorman and Thomas, 1980) and in other preparations (Petersen and Maruyama, 1984). We also detected a prolongation of the relaxation rate when the membrane was depolarized. Using a simple one-step first-order reaction scheme for calcium binding and channel opening, we deduced a halving of the closing rate (doubling of the channel open time) from 92 s^{-1} at −40 mV to 49 s^{-1} at −10 mV. The rate of channel opening may have increased ~50% with this depolarization, but this increase was not statistically significant. These changes in rate constants would lead to a threefold increase in steady-state conductance with a depolarization from −40 to −10 mV, similar to what has been reported (Gorman and Thomas, 1980).

A number of other studies on $I_{K(Ca)}$ in molluscan neurons have shown that depolarization slows the kinetics of this channel. In early studies (Heyer and Lux, 1976; Eckert and Tillotson, 1978; Lux and Hofmeier, 1982*a*), this current was activated by depolarizing the cell membrane to admit calcium through voltage-sensitive channels. Although increasing the size of depolarizing pulses slowed the rise of $I_{K(Ca)}$, this was thought to reflect the slower entry of calcium as the calcium equilibrium potential was approached. Consistent with this interpretation, Lux and Hofmeier (1982*b*) found that the activation of $I_{K(Ca)}$ by depolarizing pulses was faster when a prepulse was used to elevate intracellular calcium before the test pulse.

Voltage-dependent relaxations can properly be measured only under conditions in which intracellular calcium is constant, or changes slowly. Westerfield and Lux (1982) observed a Lorentzian component of membrane noise due to fluctuations in calcium-activated potassium current when calcium was injected iontophoretically into snail neurons. The corner frequency of this noise was between 4 and 9.5 Hz, and decreased with depolarization from 0 to +100 mV. This corresponds to relaxation rates of 60 s^{-1} at 0 mV and 25 s^{-1} at +100 mV. Hermann and Hartung (1982) reported a component of $I_{K(Ca)}$ fluctuations in snail cells of 5 Hz at −10 mV, corresponding to 31 s^{-1} relaxation rate. These estimates from noise analysis in snails are similar to our measurements in *Aplysia* when calcium was elevated by release of caged calcium.

Woolum and Gorman (1981) were the first to record the relaxation of $I_{K(Ca)}$ to voltage steps when the channels were activated by intracellular calcium injection. They found a slow component of $I_{K(Ca)}$ which relaxed at 45 s^{-1} at +34 mV and 12 s^{-1} at +114 mV in *Aplysia* neurons. These values fit reasonably well with extrapolations from our estimates of 49 s^{-1} at −10 mV and 92 s^{-1} at −40 mV. They also found a faster component, which was at least partly attributable to artefacts such as membrane capacitance discharge and potassium accumulation. Hermann and Hartung (1982) measured the relaxation of $I_{K(Ca)}$ to voltage steps after injecting calcium into snail neurons. They found a relaxation rate of 14 s^{-1} at +40 mV, 19 s^{-1} at 0 mV, and 29 s^{-1} at −40 mV. These values in snail are somewhat slower than what we observe in *Aplysia*, and what was deduced from noise analysis. They also found that the opening rate constant was virtually voltage independent. Thus, there appears to be general agreement that depolarization slows the relaxation of $I_{K(Ca)}$, mainly by prolonging the channel lifetime, with less and perhaps no effect on the opening rate.

The relaxation rate constants of Hermann and Hartung (1982) were slower than those calculated from noise analysis. They interpreted this result in terms of a two-

step reaction scheme, with receptor binding followed by several channel openings before unbinding occurred. We are certainly not able to exclude such a model. The forward and backward rates in our reaction scheme would each be influenced by receptor binding and subsequent channel opening and closing rates. The voltage dependence of the lifetime could reside in either binding or channel transition rates. Both types of voltage dependence have been proposed in models of the $I_{K(Ca)}$ from other tissues (Barrett et al., 1982; Methfessel and Boheim, 1982; Wong et al., 1982; Moczydlowski and Latorre, 1983).

Rather than try to refine molecular models of the states of the $I_{K(Ca)}$ channel, we have concentrated on how differences in the voltage dependence of $I_{K(Ca)}$ and $I_{NS(Ca)}$ can account for the different decay rates of tail currents through these channels after a depolarization. By considering both voltage-dependent relaxations and the expected calcium concentration decay after a pulse, we were able to predict the time course of $I_{K(Ca)}$ tail current. $I_{NS(Ca)}$ tail current seemed to follow the expected decline in calcium activity. The more rapid decay of the initially larger $I_{K(Ca)}$ appears to be responsible for part of the sequence of tail currents after a depolarization: For ~50 ms, $I_{K(Ca)}$ predominates at −40 mV, leading to a short-lived outward current (phase I of Kramer and Zucker, 1985*a*). This then yields to a larger $I_{NS(Ca)}$, which lasts for about 1 s (phase II of Kramer and Zucker, 1985*a*). Finally, a late outward current (phase III) is left, which decays more slowly than the others, and is due mainly to inactivation of resting calcium current (Adams and Levitan, 1985; Kramer and Zucker, 1985*b*).

The reason for the slow decay of this third phase is not yet known. We do not see evidence of a TEA-independent outward current evoked by caged calcium release in our records. It may be that the inactivation of calcium channels by calcium is less sensitive to calcium than $I_{K(Ca)}$ and $I_{NS(Ca)}$, and is normally affected only by the high local calcium concentrations in the immediate regions of calcium channel mouths (Chad and Eckert, 1984). The slow inactivation of this current may reflect the kinetics of intermediate steps which seem to involve protein phosphorylation and dephosphorylation (Eckert and Chad, 1984). An understanding of the kinetics of this last calcium-dependent current awaits analysis of these enzymatic processes.

Our discovery that the more rapid decay of $I_{K(Ca)}$ than $I_{NS(Ca)}$ is due to a differential voltage dependence may be relevant to currents in other neurons with similar differences in time course. For example, preliminary evidence (Lancaster and Adams, 1986; Lancaster and Nicoll, 1987) suggests that the different durations of two calcium-activated potassium currents in mammalian hippocampal neurons arise from a similar difference in voltage sensitivity.

APPENDIX

We describe here the structure of computational models of nitr reactions in cells.

Model I: Estimation of Surface and Volume-Average Calcium Concentrations

Step 1: equilibration of nitr and native buffer. The model begins with the concentrations of nitr and calcium injected into the cell. It is assumed that *Aplysia* neurons contain a native cytoplasmic calcium buffer with dissociation constant of 25 μM (Alemà et al., 1973). From our measured ratio of the binding efficiency of this buffer (Smith and Zucker, 1980), we

calculate its cytoplasmic concentration as 1.25–1.5 mM. For a resting calcium concentration of 200 nM (Gorman et al., 1984), this implies an additional 10 μM calcium bound to the native buffer which must be added to the calcium bound to nitr which we inject. The model proceeds to calculate the initial free calcium concentration by solving simultaneously the buffer equations for the two buffers initially present (high-affinity form of nitr and native buffer). See step 3 below for the details of these equations. We use 630 nM for the dissociation constant of nitr-5 nitrobenzhydrol in marine cytoplasm, and 213 nM for the nitr-7 high-affinity dissociation constant. These values are derived from constants measured at 100 mM ionic strength (Adams et al., 1988) and assuming the same dependence on ionic strength as measured for nitr-2 (Tsien and Zucker, 1986).

Step 2: photolysis of nitr at front surface. A light flash of a given intensity converts a fraction of the injected nitrobenzhydrol to the low-affinity nitrosobenzophenone. For example, a 200-J flash photolyzes 35% of the Ca-bound nitr and 12% of the free nitr at the front surface of the neuron. Weaker flashes photolyze proportionately less nitr. This leads to a new mixture of nitrobenzhydrol and nitrosobenzophenone at the front surface of the cell.

Step 3: reequilibration of nitr and native buffer at front surface. The free calcium concentration is recalculated by solving simultaneously buffer equations for three buffers (nitrobenzhydrol, nitrosobenzophenone, and native buffer). Let B_T, NH_T, and NP_T, represent the total concentrations of the native cytoplasmic calcium buffer, the high-affinity nitrobenzhydrol, and the low-affinity nitrosobenzophenone, and K_B, K_{NH}, and K_{NP} represent their dissociation constants for first-order binding to calcium. For nitr-5, K_{NP} = 18 μM, while for nitr-7 it is 7.7 μM. Then, following the derivation in Zucker and Steinhardt (1978), the total calcium concentration, Ca_T, is related to the free calcium concentration, Ca, by the following equation:

$$Ca_T = Ca\left[1 + \frac{B_T}{K_B + Ca} + \frac{NH_T}{K_{NH} + Ca} + \frac{NP_T}{K_{NP} + Ca}\right]. \quad \text{(A1)}$$

Solving this equation for Ca yields

$$Ca^4 + pCa^3 + qCa^2 + rCa + s = 0, \quad \text{(A2)}$$

where

$$p = K_B + K_{NH} + K_{NP} + B_T + NH_T + NP_T - Ca_T,$$

$$q = NH_T(K_{NP} + K_B) + NP_T(K_{NH} + K_B) + B_T(K_{NH} + K_{NP}) + K_{NH}K_{NP} + K_{NH}K_B + K_{NP}K_B - Ca_T(K_{NH} + K_{NP} + K_B),$$

$$r = K_{NH} + K_{NP} + K_B + NH_TK_{NP}K_B + NP_TK_{NH}K_B + B_TK_{NH}K_{NP} - Ca_T(K_{NH}K_{NP} + K_{NH}K_B + K_{NP}K_B),$$

$$s = -Ca_TK_{NH}K_{NP}K_B.$$

We used Newton's method to find the positive real root of this equation as the free calcium concentration. This calculation gives the peak calcium at the surface of the neuron facing the light source at the moment of the first flash. A simpler version of these equations, in which $NP_T = 0$, is used to estimate the initial calcium concentration in step 1.

Step 4: volume-average photolysis of nitr. The calcium concentration computed above is appropriate only for the front surface of the cell. Behind this surface, the flash intensity is reduced by absorbance as the light penetrates deeper into the cell. With a large cell filled with 10–30 mM nitr, the absorbance at 360 nm, the wavelength maximally effective in photolyzing nitr, is considerable (Tsien and Zucker, 1986). Thus, the amount of nitr converted in the cell is a function of distance from the front surface, and is nil at the back of a neuron whose diameter is 300–350 μm. Since the photolysis of nitr is linearly related to light intensity for

intensities which convert <100% of the buffer, we may calculate the average amount of nitrobenzhydrol photolyzed to nitrosobenzophenone from the average light intensity in cytoplasm. This allows us to calculate the average concentrations of high- and low-affinity forms of nitr after photolysis. Sometime after the flash, when diffusional equilibration has occurred among all the reactants (calcium, nitrobenzhydrol, nitrosobenzophenone, and native buffer), these will be the actual concentrations of the reactants everywhere in the cell. From our knowledge of the extinction coefficients of cytoplasm and the various species of nitr, we can calculate the average light intensity in a spherical neuron and from this compute the amounts of high- and low-affinity nitr present after diffusional equilibration.

To calculate the average light intensity in the cytoplasm of a spherical cell, we consider the sphere to consist of a series of cylindrical shells extending from the front surface of the cell facing the light source to the opposite surface of the neuron. The axis of each cylindrical shell passes through the center of the cell. Each shell has a radius y which runs from 0 to r, the radius of the cell. The length of each cylindrical shell is $2\sqrt{r^2 - y^2}$. If for each cylindrical shell we let $x = 0$ at the front edge of the shell, then by Beer's law the light intensity at depth x, $I(x)$, is given by

$$I(x) = Ie^{-(\epsilon \ln 10)x}, \tag{A3}$$

where I is the incident light intensity and ϵ is the overall decadic extinction coefficient of the cytoplasm containing nitr. ϵ depends on the extinction coefficient of cytoplasm, ϵ_c, and the extinction coefficients, ϵ_i, and concentrations, c_i, of the four forms of nitr (*NH*, *CaNH*, *NP*, and *CaNP*), according to

$$\epsilon = \sum_{i=1}^{4} \epsilon_i c_i + \epsilon_c. \tag{A4}$$

The average light intensity, I_{av}, in a cell of volume V is

$$I_{av} = \frac{\int I(x)\,dV}{V}. \tag{A5}$$

As volume element, dV, we use a ring of the cylindrical shell, with circumference $2\pi y$, radial thickness dy, and depth thickness dx. Since $V = 4\pi r^3/3$, Eq. A4 becomes

$$I_{av} = \frac{3}{4\pi r^3} \int_0^r 2\pi y \left[\int_0^{2\sqrt{r^2 - y^2}} Ie^{-(\epsilon \ln 10)x}\,dx \right] dy. \tag{A6}$$

Evaluating this integral, we obtain

$$I_{av}/I = \frac{3}{4G} + \frac{3}{8G^3}[(2G + 1)e^{-2G} - 1], \tag{A7}$$

where $G = r\epsilon \ln 10$.

This expression must be re-evaluated for each flash, as the nitr constituents have changed their relative concentrations due to prior flashes and the different nitr species have very different values of ϵ_i.

For in vitro calibrations using rectangular microcuvettes, Eq. A4 is simply the x-average of the expression in Eq. 3. The result is

$$I_{av}/I = \frac{1 - e^{-h\epsilon \ln 10}}{h\epsilon \ln 10}, \tag{A8}$$

where h is the path length for the photolyzing light through the tube.

For these calculations, we use the following decadic extinction coefficients for nitr-5 and

nitr-7 (kindly provided by Dr. Stephen R. Adams): Free nitrobenzhydrol, 5,780/cm·M, Ca-bound nitrobenzhydrol, 5,450/cm·M, free nitrosobenzophenone, 24,670/cm·M, and Ca-bound nitrosobenzophenone, 10,040/cm·M. We include the cytoplasmic absorbance at 360 nm, which we measured as 25/cm.

Step 5: volume-average reequilibration of nitr and native buffer. Knowing the concentrations of high- and low-affinity nitr forms after equilibration, we solve our three buffer equations again to estimate the average calcium concentration in cytoplasm following diffusional equilibration.

Step 6: calcium extrusion. The next step in our simulation is to recognize that during prolonged experiments, neurons are likely to extrude some of the excess calcium we have injected, especially that released by nitr photolysis. Calcium can be removed from cytoplasm by uptake into organelles (Blaustein et al., 1978*a*, *b*; Brinley, 1978) and by surface membrane pumps (DiPolo and Beaugé, 1983; Requena, 1983). We do not know which process dominates in *Aplysia*, but for the purpose of the present simulations it makes little difference.

We assume that calcium is removed from a neuron by a simple first-order process, such that

$$\frac{dCa}{dt} = -PCa, \tag{A9}$$

where P is the pump rate. This reduces total calcium proportionately, according to the binding ratio, or the ratio of total to free calcium, $\beta = Ca_T/Ca$. With β determined from Eq. A1, we have

$$\frac{dCa_T}{dt} = -\frac{P}{\beta}Ca. \tag{A10}$$

This leads to an exponential decline in Ca_T after a flash, approaching its final steady-state level given by

$$Ca_T(t = \infty) = \beta Ca(t = \infty), \tag{A11}$$

where $Ca(t = \infty) = 200$ nM. For flash intervals of 1–2 min, β remains constant, and we calculate the exponential decline in Ca_T until the moment of the next flash. For long intervals between flashes, β changes as Ca_T and Ca are reduced. We handle this situation by recalculating β every 1–2 min by solving Eq. 2 and adjusting the rate of dCa_T/dt according to Eq. A10.

Step 7: recalculation of free calcium concentration after extrusion. The new value of total calcium is then used to estimate the free calcium concentration after pumping, again solving simultaneously the three buffer equations by following the procedure of step 3. We are now ready to treat the effect of the next flash on surface and average nitr concentrations, and continue with step 2 of the simulation.

Model 2: Spatial and Temporal Calcium Profiles

Model 1 predicts only the peak surface calcium concentration produced by each flash, and the volume-average calcium concentration after diffusional equilibration. Model 2 extends the analysis to account for the spatial and temporal free calcium profiles following nitr photolysis. This is needed to calculate the kinetics of subsurface calcium concentration after a flash, to predict the time course of membrane currents dependent on submembrane calcium.

Step 1: photolysis of nitr as a function of distance from the cell surface. We begin with initial concentrations of *NH*, *CaNH*, *NP*, and *CaNP*. These are obtained by running Model 1 for the

number of flashes preceding the flash we wish to analyze kinetically. Since many of our results are illustrated by about the fifth flash after injection, and we usually wait about 2 min between flashes, most of our simulations assume such a history. In determining our initial conditions, we also assume that a uniform cytoplasmic calcium extrusion pump with time constant about 3.5 s has been operating in removing total calcium from injected cells. Eqs. A3 and A4 give the light intensity as a function of distance from the front surface. Since we have measured the photolysis rates of *NH* and *CaNH* for various flash intensities, we can readily calculate the percentage conversion of nitrobenzhydrol to nitrosobenzophenone at each distance behind the front surface of the cell.

Step 2: equilibration of all species at each distance from the cell surface. We now solve Eq. A2 at desired distances from the front surface to determine the concentration of calcium as a function of position in the cell. This may be used to calculate concentrations of free and bound nitr buffers and native cytoplasmic buffer at the instant of the flash.

Step 3: diffusion of all species during brief interval of time. We assume that each buffer, as well as calcium, is diffusable, and solve the diffusion equation for calcium and for free and calcium-bound forms of each of the three buffers, for a brief increment of time. We use explicit finite difference numerical solution methods (Crank, 1975), and consider diffusion to occur in one dimension in rectilinear coordinates in a closed space whose thickness equals the cell diameter. This is equivalent to representing the cell as a cube with one surface facing the light source. We usually divide the cell into 100 slices 3 μm thick. The only parameters required for this step are diffusion constants for calcium, nitr, and the native buffer. Nitr-5 free acid has a hydrated molecular weight of 776. Substances with similar molecular weight diffuse at 10^{-6} cm^2/s (or sometimes slower) in muscle (Kushmerick and Podolsky, 1969; Maylie et al., 1987). Cytoplasmic tortuosity or binding might retard diffusion somewhat, so we chose a value of 5×10^{-7} cm^2/s for the diffusion constant of all nitr species. For the native cytoplasmic buffer, we assume a diffusion constant of 10^{-7} cm^2/s. Calcium diffuses at 6×10^{-6} cm^2/s (Hodgkin and Keynes, 1957).

Step 4: successive equilibration and diffusion computations. We increment time and return to step 2 to continue with successive equilibration and diffusion calculations. For long-lasting or repeated light stimuli, each cycle of calculation also includes nitr photolysis (step 1). We usually use time increments of 5 ms, adhering to Crank's (1975) rule for the stability of finite difference solutions.

Our simulations produce data files of calcium, nitrobenzhydrol, nitrosobenzophenone, and native buffer concentrations as functions of time and distance behind the front surface.

This research was funded by National Institutes of Health grant NS-15114.

This study would not have been possible without the creative chemical developments of Prof. Roger Tsien. We thank him and Drs. Stephen Adams, Joseph Kao, and Martin Poenie for advice on the use of nitr. Mr. Russel English and Ms. Carla Pugh provided valuable technical assistance, and Dr. Francisco Alvarez-Leefmans participated in some preliminary experiments.

Original version received 10 February 1988 and accepted version received 15 September 1988.

REFERENCES

Adams, S. R., J. P. Y. Kao, G. Grynkiewicz, A. Minta, and R. Y. Tsien. 1988. Biologically useful chelators that release Ca^{2+} upon illumination. *Journal of the American Chemical Society.* 110:3212–3220.

Adams, W. B. 1985. Slow depolarizing and hyperpolarizing currents which mediate bursting in *Aplysia* neurone R15. *Journal of Physiology.* 360:51–68.

Adams, W. B., and I. B. Levitan. 1985. Voltage and ion dependences of the slow currents which mediate bursting in *Aplysia* neurone R15. *Journal of Physiology.* 360:69–93.

Ahmed, Z., and J. A. Connor. 1979. Measurement of calcium influx under voltage clamp in molluscan neurones using the metallochromic dye arsenazo III. *Journal of Physiology.* 286:61–82.

Alemà, S., P. Calissano, G. Rusca, and A. Giuditta. 1973. Identification of a calcium-binding, brain specific protein in the axoplasm of squid giant axons. *Journal of Neurochemistry.* 20:681–689.

Barish, M. E., and S. H. Thompson. 1983. Calcium buffering and slow recovery kinetics of calcium-dependent outward current in molluscan neurones. *Journal of Physiology.* 337:201–219.

Barrett, J. N., K. L. Magleby, and B. S. Pallotta. 1982. Properties of single calcium-activated potassium channels in cultured rat muscle. *Journal of Physiology.* 331:211–230.

Blaustein, M. P., R. W. Ratzlaff, and N. K. Kendrick. 1978*a*. The regulation of intracellular calcium in presynaptic nerve terminals. *Annals of the New York Academy of Sciences.* 307:195–212.

Blaustein, M. P., R. W. Ratzlaff, and E. S. Schweitzer. 1978*b*. Calcium buffering in presynaptic nerve terminals. II. Kinetic properties of the nonmitochondrial Ca sequestration mechanism. *Journal of General Physiology.* 72:43–66.

Brinley, F. J., Jr. 1978. Calcium buffering in squid axons. *Annual Review of Biophysics and Bioengineering.* 7:363–392.

Brown, A. M., and D. L. Kunze. 1974. Ionic activities in identifiable *Aplysia* neurons. *In* Ion-Selective Microelectrodes. H. J. Berman and N. C. Hebert, editors. Plenum Publishing Corp., New York. 57–68.

Chad, J. E., and R. Eckert. 1984. Calcium domains associated with individual channels can account for anomalous voltage relations of Ca-dependent responses. *Biophysical Journal.* 45:993–999.

Chad, J., R. Eckert, and D. Ewald. 1984. Kinetics of calcium-dependent inactivation of calcium current in voltage-clamped neurones of *Aplysia californica. Journal of Physiology.* 347:279–300.

Crank, J. 1975. *The Mathematics of Diffusion.* 2nd edition. Oxford University Press, Oxford.

DiPolo, R., and L. Beaugé. 1983. The calcium pump and sodium-calcium exchange in squid axons. *Annual Review of Physiology.* 45:313–324.

Eckert, R., and J. E. Chad. 1984. Inactivation of Ca channels. *Progress in Biophysics and Molecular Biology.* 44:215–267.

Eckert, R., and D. Ewald. 1982. Residual calcium ions depress activation of calcium-dependent current. *Science.* 216:730–733.

Eckert, R., and D. Tillotson. 1978. Potassium activation associated with intraneuronal free calcium. *Science.* 200:437–439.

Ewald, D. A., A. Williams, and I. B. Levitan. 1985. Modulation of single Ca^{2+}-dependent K^+-channel activity by protein phosphorylation. *Nature.* 315:503–506.

Findlay, I., M. J. Dunne, and O. H. Petersen. 1985. High-conductance K^+ channel in pancreatic islet cells can be activated and inactivated by internal calcium. *Journal of Membrane Biology.* 83:169–175.

Gorman, A. L. F., and A. Hermann. 1982. Quantitative differences in the currents of bursting and beating molluscan pace-maker neurones. *Journal of Physiology.* 333:681–699.

Gorman, A. L. F., A. Hermann, and M. V. Thomas. 1982. Ionic requirements for membrane oscillations and their dependence on the calcium concentration in a molluscan bursting pace-maker neurone. *Journal of Physiology.* 327:185–217.

Gorman, A. L. F., S. Levy, E. Nasi, and D. Tillotson. 1984. Intracellular calcium measured with calcium-sensitive micro-electrodes and arsenazo III in voltage-clamped *Aplysia* neurones. *Journal of Physiology.* 353:127–142.

Gorman, A. L. F., and M. V. Thomas. 1978. Changes in the intracellular concentration of free calcium ions in a pace-maker neurone, measured with the metallochromic indicator dye arsenazo III. *Journal of Physiology.* 275:357–376.

Gorman, A. L. F., and M. V. Thomas. 1980. Potassium conductance and internal calcium accumulation in a molluscan neurone. *Journal of Physiology.* 308:287–313.

Graubard, K. 1975. Voltage attenuation within *Aplysia* neurons: the effect of branching pattern. *Brain Research.* 88:325–332.

Gurney, A. M., R. Y. Tsien, and H. A. Lester. 1987. Activation of a potassium current by rapid photochemically generated step increases of intracellular calcium in rat sympathetic neurons. *Proceedings of the National Academy of Science.* 84:3496–3500.

Hermann, A., and A. L. F. Gorman. 1981. Effects of tetraethylammonium on potassium currents in a molluscan neuron. *Journal of General Physiology.* 78:87–110.

Hermann, A., and K. Hartung. 1982. Noise and relaxation measurements of the Ca^{2+} activated K^+ current in Helix neurones. *Pflügers Archiv.* 393:254–261.

Heyer, C. B., and H. D. Lux. 1976. Control of the delayed outward potassium currents in bursting pace-maker neurones of the snail, *Helix pomatia. Journal of Physiology.* 262:349–382.

Hodgkin, A. L., and A. F. Huxley. 1952. A quantitative description of membrane current and its application to conduction and excitation in nerve. *Journal of Physiology.* 117:500–544.

Hodgkin, A. L., and R. D. Keynes. 1957. Movements of labelled calcium in squid giant axons. *Journal of Physiology.* 138:253–281.

Hofmeier, G., and H. D. Lux. 1981. The time courses of intracellular free calcium and related electrical effects after injection of $CaCl_2$ into neurons of the snail, *Helix pomatia. Pflügers Archiv.* 391:242–251.

Kostyuk, P. G., P. A. Doroshenko, and A. Y. Tsyndrenko. 1980. Calcium-dependent potassium conductance studied on internally dialysed nerve cells. *Neuroscience.* 5:2187–2192.

Kramer, R. H., and R. S. Zucker. 1985*a*. Calcium-dependent inward current in *Aplysia* bursting pace-maker neurones. *Journal of Physiology.* 362:107–130.

Kramer, R. H., and R. S. Zucker. 1985*b*. Calcium-induced inactivation of calcium current causes the inter-burst hyperpolarization of *Aplysia* bursting neurones. *Journal of Physiology.* 362:131–160.

Kushmerick, M. J., and R. J. Podolski. 1969. Ionic mobility in muscle cells. *Science.* 166:1297–1298.

Lancaster, B., and P. R. Adams. 1986. Calcium-dependent current generating the afterhyperpolarization of hippocampal neurons. *Journal of Neurophysiology.* 55:1268–1281.

Lancaster, B., and R. A. Nicoll. 1987. Properties of two calcium-activated hyperpolarizations in rat hippocampal neurones. *Journal of Physiology.* 389:187–203.

Lux, H. D., and G. Hofmeier. 1982*a*. Properties of a calcium- and voltage-activated potassium current in Helix pomatia neurons. *Pflügers Archiv.* 394:61–69.

Lux, H. D., and G. Hofmeier. 1982*b*. Activation characteristics of the calcium-dependent outward potassium current in Helix. *Pflügers Archiv.* 394:70–77.

Lux, H. D., E. Neher, and A. Marty. 1981. Single channel activity associated with the calcium-dependent outward current in *Helix pomatia. Pflügers Archiv.* 389:293–295.

Maylie, J., M. Irving, N. L. Sizto, and W. K. Chandler. 1987. Comparison of arsenazo III optical signals in intact and cut frog twitch fibers. *Journal of General Physiology.* 89:41–81.

Meech, R. W., and R. C. Thomas. 1980. Effect of measured calcium chloride injections on the membrane potential and internal pH of snail neurones. *Journal of Physiology.* 298:111–129.

Methfessel, C., and G. Boheim. 1982. The gating of single calcium-dependent potassium channels is described by an activation/blockade mechanism. *Biophysics of Structure and Mechanism.* 9:35–60.

Moczydlowski, E., and R. Latorre. 1983. Gating kinetics of Ca^{2+}-activated K^+ channels from rat muscle incorporated into planar lipid bilayers. Evidence for two voltage-dependent Ca^{2+} binding reactions. *Journal of General Physiology.* 82:511–542.

Petersen, O. H., and Y. Maruyama. 1984. Calcium-activated potassium channels and their role in secretion. *Nature.* 307:693–696.

Requena, J. 1983. Calcium transport and regulation in nerve fibers. *Annual Review of Biophysics and Bioengineering.* 12:237–257.

Requena, J., and L. J. Mullins. 1979. Calcium movement in nerve fibres. *Quarterly Review of Biophysics.* 12:371–460.

Smith, S. J., and S. H. Thompson. 1987. Slow membrane currents in bursting pace-maker neurones of *Tritonia. Journal of Physiology.* 382:425–448.

Smith, S. J., and R. S. Zucker. 1980. Aequorin response facilitation and intracellular calcium accumulation in molluscan neurones. *Journal of Physiology.* 300:167–196.

Swandulla, D., and H. D. Lux. 1985. Activation of a nonspecific cation conductance by intracellular Ca^{2+} elevation in bursting pacemaker neurons of *Helix pomatia. Journal of Neurophysiology.* 54:1430–1443.

Thompson, S. H., and R. W. Aldrich. 1980. Membrane potassium channels. *In* The Cell Surface and Neuronal Function. C. W. Cotman, G. Poste, and G. L. Nicolson, editors. Elsevier Science Publishing Co., Inc., New York, 49–85.

Thompson, S. H., and S. J. Smith. 1976. Depolarizing afterpotentials and burst production in molluscan pacemaker neurons. *Journal of Neurophysiology.* 39:153–161.

Tsien, R., and R. S. Zucker. 1986. Control of cytoplasmic calcium with photolabile 2-nitrobenzhydrol tetracarboxylate chelators. *Biophysical Journal.* 50:843–853.

Vergara, C., and R. Latorre. 1984. Kinetics of Ca^{2+}-activated K^+ channels from rabbit muscle incorporated into planar bilayers: evidence for a Ca^{2+} and Ba^{2+} blockade. *Journal of General Physiology.* 82:543–568.

Westerfield, M., and H. D. Lux. 1982. Calcium-activated potassium conductance noise in snail neurons. *Journal of Neurobiology.* 12:507–517.

Wong, B. S., H. Lecar, and M. Adler. 1982. Single calcium-dependent potassium channels in clonal anterior pituitary cells. *Biophysical Journal.* 39:313–317.

Woolum, J. C., and A. L. F. Gorman. 1981. Time dependence of the calcium-activated potassium current. *Biophysical Journal.* 36:297–302.

Zucker, R. S. 1981. Tetraethylammonium contains an impurity which alkalizes cytoplasm and reduces calcium buffering in neurons. *Brain Research.* 208:473–478.

Zucker, R. S. 1982. Stray light correction for microspectrophotometric determination of intracellular ion concentration. *Journal of Neuroscience Methods.* 5:389–394.

Zucker, R. S., and S. J. Smith. 1979. Effect of TEA on light emission from aequorin-injected Aplysia central neurons. *Brain Research.* 169:91–102.

Zucker, R. S., and R. A. Steinhardt. 1978. Prevention of the cortical reaction in fertilized sea urchin eggs by injection of calcium-chelating ligands. *Biochimica et Biophysica Acta.* 541:459–466.